



Deliverable 3.2

Final Case Study Report on Improved Localization of Seismic Events, Denmark, The Netherlands, Iceland, Including Recommendations for Improved Monitoring and Localization of Seismic Events in other Regions of Europe

Authors and affiliation:

Tine B. Larsen, GEUS
Sigríður Kristjánsdóttir, ISOR
Joana Esteves Martins, TNO
Peter H. Voss, GEUS
Trine Dahl-Jensen, GEUS
Niels Hemmingsen Schovsbo, GEUS

E-mail of lead author:
tbl@geus.dk

Version: 2021.10.14

This report is part of a project that has received funding by the European Union's Horizon 2020 research and innovation programme under grant agreement number 731166. Scientific work is co-funded by the Geological Surveys and national funds allocated for science within the period 2018-2021.



Deliverable Data		
Deliverable number	D3.2	
Dissemination level	General Public	
Deliverable name	Final Case Study Report on Improved Localization of Seismic Events, Denmark, The Netherlands, Iceland, Including Recommendations for Improved Monitoring and Localization of Seismic Events in other Regions of Europe	
Work package	WP3, Hazard and Impacts Method Development	
WP Lead /Deliverable beneficiary	GEUS/GEUS	
Deliverable status		
Submitted (Author(s))	28/09/2021	T. Larsen, S. Kristjánsdóttir, J. Esteves Martins, P. Voss, T. Dahl-Jensen, N. Hemmingsen Schovsbo
Reviewed/Verified(WP leader)	04/10/2021	Hideo Aochi [BRGM], T. Larsen (GEUS)
Approved (Project leader)	14/10/2021	Hans Doornenbal [TNO]



TABLE OF CONTENTS

1	INTRODUCTION	2
1.1	Document Background and Scope	2
1.2	Abbreviations.....	2
1.3	HIKE WP3 contributors.....	3
2	HIKE WP3 CASE STUDY AMBITIONS AND EXPECTED IMPACTS.....	4
2.1	The case study concept.....	4
2.2	Summary of case study technologies	4
3	OBJECTIVES OF THE CASE STUDY ON ADVANCED LOCALIZATION OF SEISMICITY	5
4	SUMMARY/ABSTRACT.....	6
5	KEYWORDS.....	7
6	GEOLOGICAL SETTING	8
7	CASE STUDY ENERGY EXPLOITATION/STORAGE	15
8	METHODOLOGY.....	16
9	ANALYSIS, DISCUSSION AND UNCERTAINTY EVALUATION	19
10	POTENTIAL IMPACT	28
11	IMPORTANCE OF FAULT DATABASE TO IMPROVED HYPOCENTER DETERMINATION METHODOLOGY	29
12	CROSS-CUTTING RELATIONS BETWEEN CASE STUDIES.....	30
12.1	Cross-cutting: uncertainty estimates.....	30
12.2	Cross-cutting: Scientific basis for further operations	30
13	BEST PRACTICE WITHIN THE FIELD OF EARTHQUAKE LOCATION AND MONITORING	32
14	RELEVANCE OF THIS STUDY TO THE NEW GREEN DEAL AND PROPOSED FUTURE STUDIES.....	33
15	REFERENCES	34
16	SUPPLEMENTARY MATERIAL: FIRST STEPS IN NONLINLOC.....	37



1 INTRODUCTION

1.1 Document Background and Scope

This document is the final HIKE WP3, T3.1 report. The document contains a description of the case study methodology, case study settings, and work carried out during this project. In addition to the individual contribution of T3.1, this document also focusses on possible interaction with the HIKE European Fault database (FDB) and cross cutting relations between case studies. It is the objective to give an in-depth description of the individual case studies, and show the way forward for future work.

1.2 Abbreviations

HIKE	= Project "Hazards and Impacts Knowledge Europe"
GIP	= Project "Geo-Information Platform"
EGS	= EuroGeoSurveys organization
GEEG	= Geo-Energy Expert Group (EGS)
EOEG	= Earth Observation Expert Group (EGS)
MREG	= Mineral Resources Expert Group (EGS)
WREG	= Water Resources Expert Group (EGS)
SIEG	= Spatial Information Expert Group (EGS)
EC	= European Commission
MS	= Member States
NGO	= Non-Governmental Organization
EGDI	= European Geo Data Information Platform
DMP	= Data Management Plan
PIP	= Project Implementation Plan
PMB	= Project Management Board (project lead + work package leads)
PA	= Project Assembly
PL	= Project Lead
WPL	= Work Package Lead
TL	= Task Lead
CDE	= Communication, Dissemination and Exploitation (plan)
FDB	= Fault database
HIDB	= Hazard and Impacts database
SHARE	= Project "Seismic Hazards Research Europe"
EPOS	= Project "European Plate Observing System"
MICA	= Project "Mineral Intelligence Capacity Analysis"
DOI	= Digital Object Identifier
GSO	= Geological Survey Organization
INSPIRE	= Infrastructure for Spatial Information in Europe
GEOSCIML	= data model and data transfer standard for geological data
SI	= International System of Units



1.3 HIKE WP3 contributors

#	Participant Legal Name	Institution	Country
1	Nederlandse Organisatie voor Toegepast Natuurwetenschappelijk Onderzoek TNO	TNO (coordinator)	Netherlands
2	Albanian Geological Survey	AGS	Albania
3	Geologische Bundesanstalt	GBA	Austria
4	Royal Belgian Institute of Natural Sciences – Geological Survey of Belgium	RBINS-GSB	Belgium
5	Geological Survey of Denmark and Greenland	GEUS	Denmark
6	Bureau de Recherches Géologiques et Minières	BRGM	France
7	Bundesanstalt für Geowissenschaften und Rohstoffe	BGR	Germany
8	Landesamt für Bergbau, Geologie und Rohstoffe Brandenburg	LBGR	Germany
9	Landesamt für Geologie und Bergwesen Sachsen-Anhalt	LAGB	Germany
10	Bayerisches Landesamt für Umwelt	LfU	Germany
11	Islenskar orkurannsoknir - Iceland GeoSurvey	ISOR	Iceland
12	Istituto Superiore per la Protezione e la Ricerca Ambientale	ISPRA	Italy
13	Servizio Geologico, Sismico e dei Suoli della Regione Emilia-Romagna	SGSS	Italy
14	Agenzia Regionale per la Protezione Ambientale del Piemonte	ARPAP	Italy
15	Lietuvos Geologijos Tarnyba prie Aplinkos Ministerijos	LGT	Lithuania
16	Państwowy Instytut Geologiczny – Państwowy Instytut Badawczy	PIG-PIB	Poland
17	Laboratório Nacional de Energia e Geologia	LNEG	Portugal
18	Geološki zavod Slovenije	GeoZS	Slovenia
19	State Research and Development Enterprise State Information Geological Fund of Ukraine	GEOINFORM	Ukraine



2 HIKE WP3 CASE STUDY AMBITIONS AND EXPECTED IMPACTS

2.1 The case study concept

HIKE WP3 has developed and tested novel methodologies building on top of results from previous projects and research. The work has advanced current state-of-the-art knowledge across different energy exploitation scenarios and various geological settings. The final goal is to improve hazard and impact assessments and provide the basis for better standardization of these evaluations across Europe. With the joint development of methods, workflows and datasets an intensified research collaboration and improved transfer of knowledge has been established.

Different types of energy exploitation of the subsurface give rise to different challenges. These include, but are not limited to: induced seismicity, induced subsidence, as well as reservoir sealing and leakage. The processes are to a varying degree relevant for both energy extraction and subsurface storage. A common theme for these hazards is the importance of faults. Faults can guide subsurface motion as well as provide pathways for leakage. Furthermore, faults can be activated due to changes in external conditions such as pressure changes and lubrication by liquids.

Based on the participating partners' expertise four case studies have been formulated to cover as broad a range of methodologies as possible. In all case studies the relevance of the fault database being established in WP2 will be explored. Furthermore, cross-cutting relations between individual case studies will be identified. The outcome of the case studies will be made publicly available through the share point in WP4 and through relevant meetings and publications.

2.2 Summary of case study technologies

- Advanced localization of seismic events in Europe; Denmark, Netherlands and Iceland case studies
- Evaluation of methodologies for induced surface displacements; Po Basin, Italy case study
- Development and application of novel methods for reservoir sealing assessment; Poland case study
- Assessment of seismicity and safety in storage, Lacq Rousse, France case study



3 OBJECTIVES OF THE CASE STUDY ON ADVANCED LOCALIZATION OF SEISMICITY

Earthquakes carry important information on the current state of stress in the subsurface as well as information about the location of weaknesses. Energy exploitation activities and energy storage are inherently connected to changes in pressure in the subsurface. Different pressure changes are applied depending on the level of activity. Especially rapid changes in pressure are known to lead to induced and triggered earthquakes (Ellsworth, 2013; Bommer et al, 2015) and in some cases lead to reactivation of otherwise stable and unknown faults (Horton, 2012). Even smaller felt earthquakes can generate considerable interest and concern in the general public and in some cases, increased small magnitude seismicity is an indication of possible larger events to follow e.g., Basel (Deichmann & Giardini, 2009; Terakawa et al., 2012), Oklahoma, (Schoenball & Ellsworth, 2017). Wilson et al., 2017 attempts to maintain a database of induced earthquakes at <https://inducedearthquakes.org/>

Using small magnitude earthquakes as a first warning system in energy exploitation is quite common, especially in the form of the so-called Traffic Light System (TLS), (e.g., Cherry et al, 2015; de Pater & Baisch, 2011). However, the performance of the warning system is depending on the quality of the earthquake monitoring system. Small earthquakes can be elusive and hard to locate precisely due to low signal-to-noise levels, insufficient number of seismograph stations as well as over simplified methods and subsurface models. These challenges need to be overcome to be able to more accurately relate microseismicity to anthropogenic activities, and to be able to relate earthquakes to individual faults – both known faults and faults previously unknown.

Discerning anthropogenic events from natural earthquakes is also a challenge where precise hypocenter determination is of great value in concert with other methods such as surface deformation and stress field modeling. An example of a pair of earthquakes that caused great concern in relation to subsurface exploitation is the Emilia-Romagna, Italy, Mw 5.9 and Mw 5.8 earthquakes near the Cavone Oil Field in 2012. The lack of a local seismic network for precise hypocenter determination caused a five-year long debate over the nature of these events. They were eventually characterized as natural, tectonic earthquakes. See Albano et al, 2017 and references therein.

The main objective of T3.1 is to explore ways to improve the localization of earthquakes as a) anthropogenic earthquakes can be a first warning sign of problems in energy exploitation and subsurface storage, b) precise locations can in some cases link earthquakes to specific faults, c) precise locations can in some cases reveal sleeping or unknown faults waking up, d) there is a need to improve the capability to discern between natural and induced/triggered events.

Ultimately improved localization of earthquakes will contribute to improving the basis for hazard and impact assessments for subsurface energy exploitation and storage projects and contribute to a better scientific basis for standardization of these assessments across Europe. Reduced uncertainty on locations can also lead to more efficient mitigation during subsurface activities.



4 SUMMARY/ABSTRACT

Improved determination of hypocenter solutions can be achieved in several different ways: a) improved recording of the events, b) improved velocity models, and c) improved analytical methods. In this report we have explored aspects of all three approaches.

Incorporating data from Ocean Bottom Seismometers (OBS) when locating offshore earthquakes has the potential to improve hypocenter precision. Data from the seabed have been shown to be of a high quality with high signal-to-noise ratio, and the data has successfully been combined with data from land-based seismographs. However, there are several challenges related to OBS data: the instruments do not have connection to satellites during deployment, and the time stamps on the data are dependent on the internal clock of the instruments. The internal clock is drifting and the absolute times of P- and S-wave arrivals cannot be used. Instead the differential P-S time is used in the analysis. The lack of realtime data from an OBS makes it unsuitable as a component in a mitigation system, but shows great promise for improved hypocenter determination when realtime solutions are not required.

Locating an earthquake recorded on a network of seismographs involves solving the wave equation for P- and S-waves propagating through the subsurface. The velocity model is a critical a priori parameter, and the solution is highly dependent on the quality of the model. Applying station corrections to a 1D velocity model has been demonstrated to improve the hypocenter solutions, placing them closer to known faults with less scatter in the locations, both horizontally and vertically. Likewise, an improved velocity model based on local data can reduce the scatter.

The least successful part of the investigation was to test the non-linear Monte Carlo based analysis software NonLinLoc. The software turned out to be very difficult to get to work properly, in particular the choice of grids for the velocity model as well as the search grid for the solution were non-trivial. However, good results were obtained in Iceland. Further work is needed to explore and master the full potential of this method.



5 KEYWORDS

Seismicity, earthquakes, hypocentre, velocity model, induced seismicity, triggered seismicity



6 GEOLOGICAL SETTING

Geological setting Danish case study:

The Study area lies within the Danish-Norwegian Basin that is an intra-cratonic, Permian–Cenozoic structure that trends WNW–ESE bounded by basement blocks of the Ringkøbing–Fyn High to the south and by the Fennoscandian Border Zone to the north-east (Nielsen 2003; Figure 1). The area has been studied though many decades and the present summary is mainly based on Vejgåk (1997), Nielsen (2003) and Lassen & Tybo (2012).

The area to the northwest represents the transition to the stable Precambrian Baltic Shield and includes the Sorgenfrei–Tornquist Zone and the Skagerrak–Kattegat Platform (Figure 1). The Sorgenfrei–Tornquist Zone itself forms the northern segment of the Tornquist Zone that is a long-lived tectonic feature that extends across Europe. It thus converges with the Teisseyre–Tornquist Zone in the Rønne Graben offshore Bornholm, where the Danish Basin grades into the Polish Trough. The Sorgenfrei–Tornquist Zone is heavily block-faulted, 30–50 km wide, with tilted Palaeozoic fault blocks that are unconformably overlain by thick Mesozoic deposits (Vejgåk 1997; Nielsen 2003; Lassen & Tybo 2012). These shows pronounced late Cretaceous – early Cenozoic tectonic inversion. The Skagerrak–Kattegat Platform is a stable area to the north-east where the Mesozoic deposits onlap lower Permian, lower Palaeozoic, and Precambrian crystalline rocks in tilted fault blocks and gradually thin out towards the Baltic Shield (Nielsen 2003).

The deepest most reliable regional surface mappable by reflection seismic data in the Danish Basin and Fennoscandian Border Zone is the top pre-Zechstein surface, which is a pronounced unconformity truncating tilted fault blocks in most of the area (Vejgåk 1997, Lassen & Tybo 2012). The unconformity is penetrated by wells that document the occurrence of Precambrian crystalline rocks on the Ringkøbing–Fyn High (Nielsen 2003) and the Skagerrak–Kattegat Platform and Lower Palaeozoic sedimentary rocks in the Danish Basin and Fennoscandian Border Zone (see summary by Nielsen 2003).

Deeper regional surfaces have been mapped representing the “near” top-crystalline basement reflector, thickness of the middle to lower Palaeozoic sedimentary interval, depth to Moho, and thickness of the crystalline crust (Lassen & Tybo 2021). These maps show a generally strongly faulted Precambrian basement surface below several thick pre-Permian basins, most notably on the East North Sea High.

Lassen & Tybo (2012) did not identify the “basement” reflection directly in large parts of the study area. Instead a pronounced seismic interface from sandstone to shale could be imaged ~300 m above the crystalline basement. Rift sequences of inferred late Ediacaran to early Cambrian ages was interpreted to be present in Kattegat (up to ~800 m thick), in the SW Baltic Sea (up to ~2000 m thick) (Lassen & Tybo 2012). The study also documents that the tilted fault block crests are deeply truncated by the mid-Permian unconformity showing that regional post-rift thermal subsidence was somewhat delayed as suggested by Vejgåk (1997). The unconformity defines the base of the post-rift succession and is in the Danish-Norwegian basin overlain by a relatively complete succession of upper Permian, Mesozoic and Cenozoic deposits that is c. 5–6.5 km thick along the basin axis and more than 9 km locally.

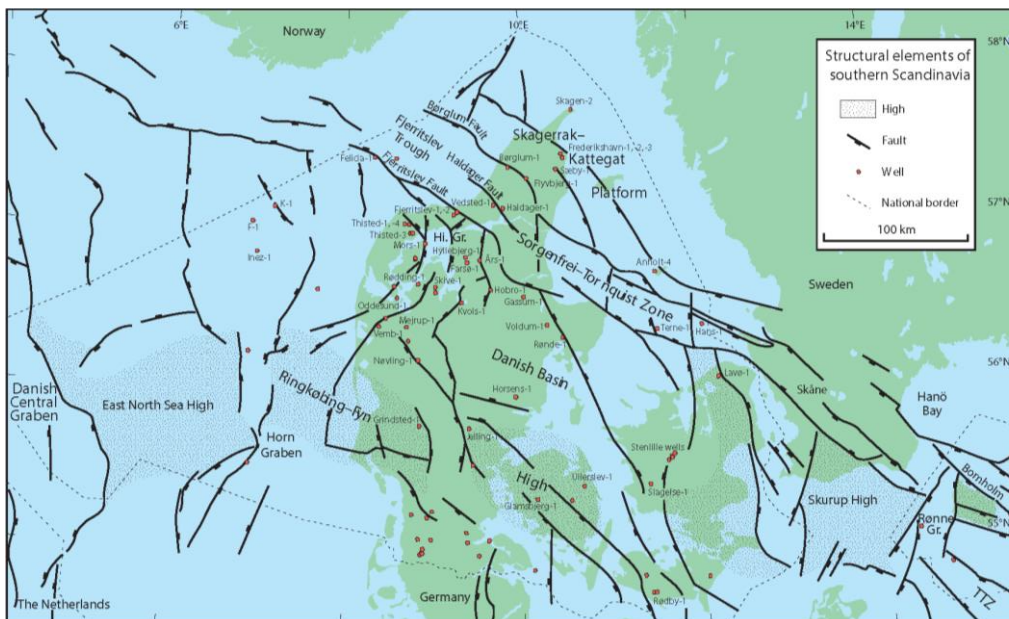


Figure 1: Structural map of the Danish area. From Nielsen (2003).

Geological setting Dutch case study:

Owing to the large hydrocarbon exploration history, and efforts of the The Geological Survey of the Netherlands (TNO) to better understand the deep subsurface of the on- and offshore areas, the subsurface is one of the most well-known. Below the flat topography, siliciclastic sediments with almost continuous records since late Paleozoic, overlie a metamorphic basement [Dienst, Rijks Geologische, 1994]. The sedimentary layers have been highly affected by several tectonic events until the present time, forming major unconformities such as basins, platforms and peaks [Jager et al., 2007, Duin et al., 2006, Kombrink et al., 2012 amongst others]

Jager et al., summarized the most important tectonic event originating such unconformities as such: (i) the Caledonian and Variscan orogenies, resulting in the assembly of the Pangea supercontinent during the Paleozoic, (ii) Mesozoic rifting, accompanying the break-up of Pangea, (iii) Alpine inversion, resulting from the collision of Africa and Europe during the Late Cretaceous and Early Tertiary, and (iv) Oligocene to recent development of the Rhine Graben rift system (Wong et al., 2007).

The Netherlands (NL) structured subsurface due to the just referred tectonic events resulted in a varied geology with prominent structural domains. These domains are described by Jager et al. (2007) and the references herein, as late Jurassic to Early Cretaceous extensional and transtensional rift basins, viz. the Dutch Central Graben, the Broad Fourteens Basin, the West and Central NL basins, the Roer Valley Graben and the Lower Saxony Basin (Figure 1).

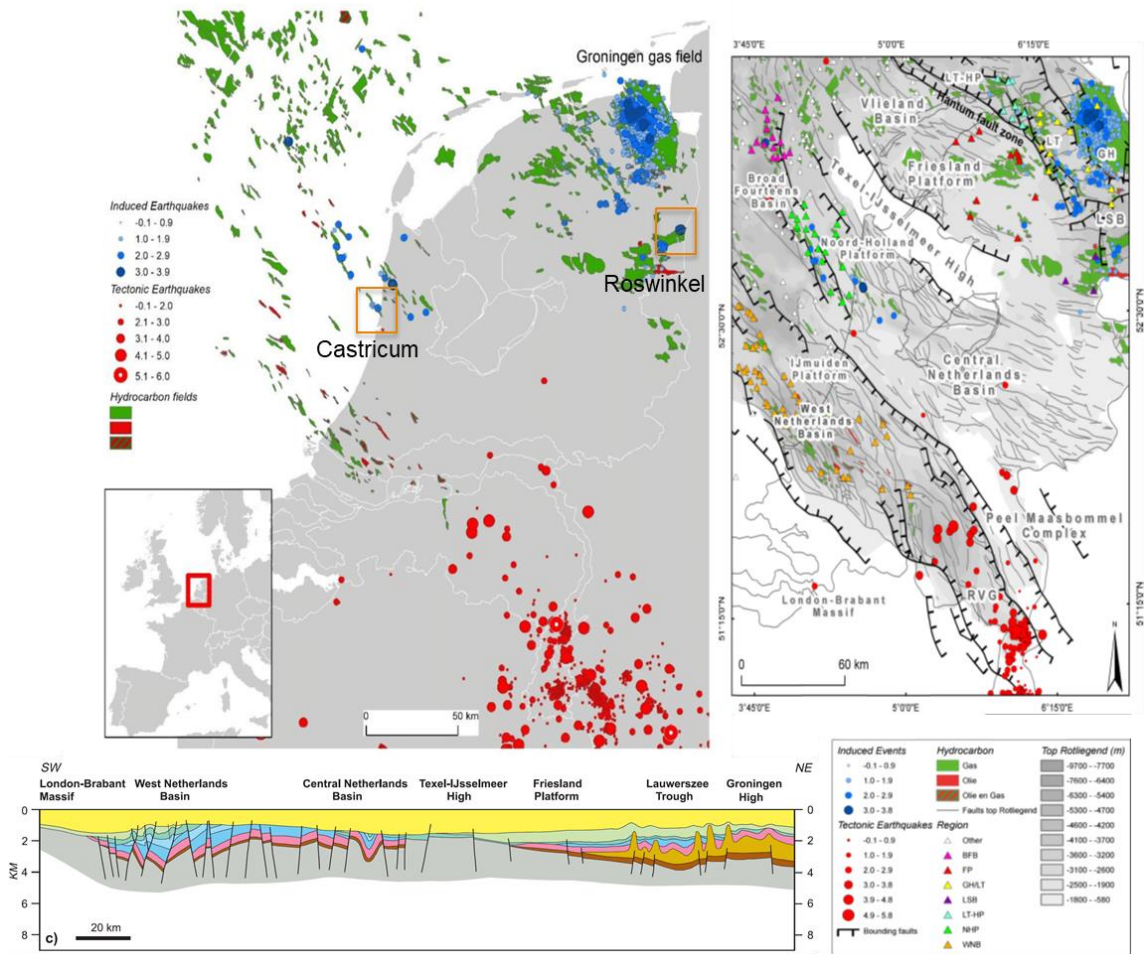


Figure 2 – Top-left: Overview of The Dutch tectonic setting, induced (blue circles) and natural (red circles) seismicity up to 2020 on top of some gas reservoirs (adapted from Buijze, [2020]). Top-right: Main structural domains with seismicity (KNMI up to 2012), adapted from Van Wees et al.2014, after Wong et al.,2007 KNMI (2012), NLOG (2012) for depth of top Rotliegend,gas fields and regional faults at the level of the Lower Triassic. Hydrocarbon reservoirs are indicated in green (gas) and red (oil). Major fault zones (solid black lines) separate the main tectonic elements which characterize the subsurface of the Netherlands after Jager et al., 2007. Local faults are plotted in grey. The nomenclature of the fault structures extended and not extended in the figure corresponds to: BFB =Broad Fourteen Basin, FP=Friesland Platform, GH/LT=Groningen High/Lauwerszee Trough, LSB=Lower Saxony Basin, LT/HP=Lauwerszee trough-Hantum Platform, NHP=Noord Holland Platform, WNB=West Netherlands Basin. RVG=Roer Valley Graben, PB=Peelrand Block, EL=Ems Low. Bottom left: Cross-section of the NL geology from SW to NE showing the mentioned unconformities and structural domains (adapted from Jager et al., 2007). Bottom-right: legend.

Two types of seismicity have been identified with a clear separation between the north of the country where over 190 gas fields of varying size have been exploited, and the south, which is considered to be more tectonically active (Figure 2). Nevertheless, Van Wees et al. [2014] estimated that no more than 15% of these fields show seismicity and geomechanical studies show that largest seismicity is localized on pre-existing fault structures.



For the Dutch case studies, we have chosen two decommissioned gas fields where seismicity occurred after the end of production: the Roswinkel and Castricum gas fields. With new initiatives to re-use old decommissioned gas fields to energy or CO₂ storage together with the fact that seismicity is still occurring at one of the decommissioned gas fields, the exact location and event uncertainty of the seismic events is of high importance.

Roswinkel

The Roswinkel gas field (Figure 3) is located at about 2100 m depth, in the northeast of the Netherlands (south of the known Groningen gas field) with nearly 25 years of production from 1980 to 2005. The gas field is characterized by dense faulting, high field compartmentalization (with approximately 30 reservoir compartments), and with induced subsidence of roughly 17 cm above the centre of the field [Fokker, 2012]. Seismicity around Roswinkel gasfield has been recorded in the mid-1990s and early 2000s, reaching the maximum magnitude of 3.4 and with seismic event occurrences even after the end of production also though the field complexity may introduce difficulties in the event location, the well-known subsurface and well-constrained 3D velocity model at this location because of the existence of 8 wells producing from the field.

Even though the events recorded in early 2000's reached a magnitude of 3.4 and would therefore be interesting to relocate with a 3D velocity model, the seismic network was not optimal. Because of this reason, during the Hike project we decided to drop the relocation of the Roswinkel events.

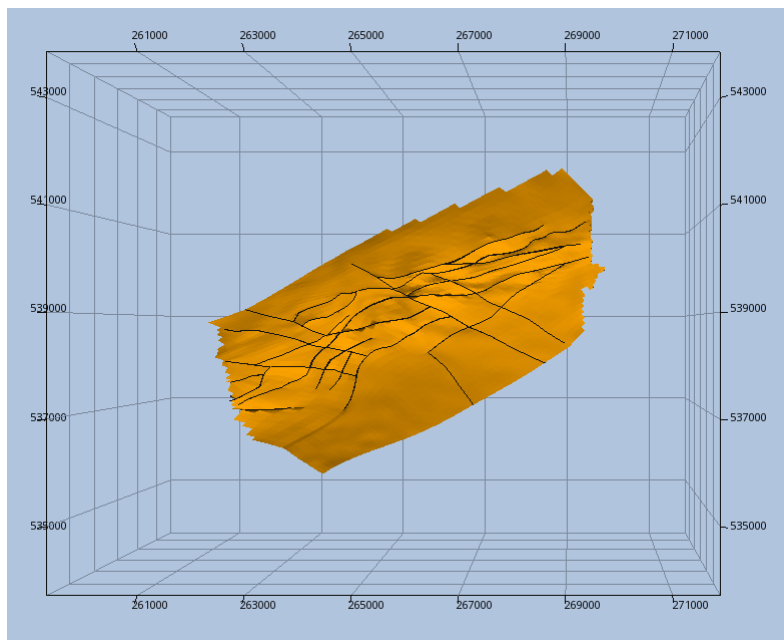


Figure 3 – Roswinkel gas reservoir with the corresponding identified faults and reservoir compartments (adapted after Fokker et al., 2012).



Castricum

In 2013, five earthquakes near Castricum (Figure 4) in the North Sea were registered by the KNMI (Koninklijk Nederlands Meteorologisch Instituut) seismic network. The first registered earthquake had the highest magnitude (2.5 on the Richter scale) followed by five other lower magnitude events with no seismicity observed in this area since then. The locations of the quakes, in the vicinity of the Castricum-Sea gas field, suggests that the earthquakes may be related to the depletion of this gas field (in production between 2000 and 2004). Because part of the gas reservoir is offshore, a limitation we find for this Area of Interest (AOI) is the location of the seismometers, nevertheless given that there is a 3D velocity model available for the whole country we used this case study as our main focus.

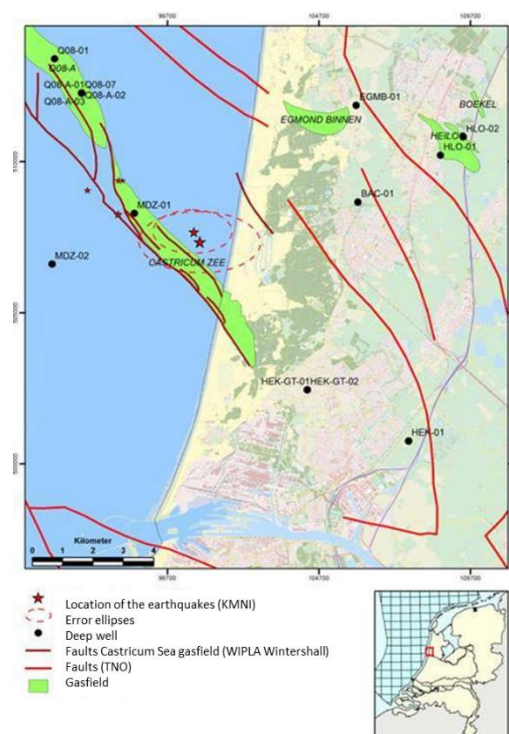


Figure 4. Events near Castricum located by KNMI in 2013, with a more complete KNMI seismic network. Two events were located far from known faults but the uncertainty in the two events location (red ellipses) can lead to association with existing known faults. The red stars locate the events, the green polygons locate the gas fields and the red lines the faults identifies in the area (adapted from TNO, 2013).

One of these events, in October 22, 2013 occurred under the North Sea west of Castricum. The quake was shallow, about 3 km, and had a magnitude of 2.5 on the Richter scale. In October 23 another quake had a magnitude of 2.0 on the Richter scale and a depth of approximately 3 km.

KNMI has received 250 reports from people who have felt vibrations, especially from Castricum, Egmond-binnen and Limmen underlining the importance of understanding if the origin of these events are lingering effects of previous gas operations.

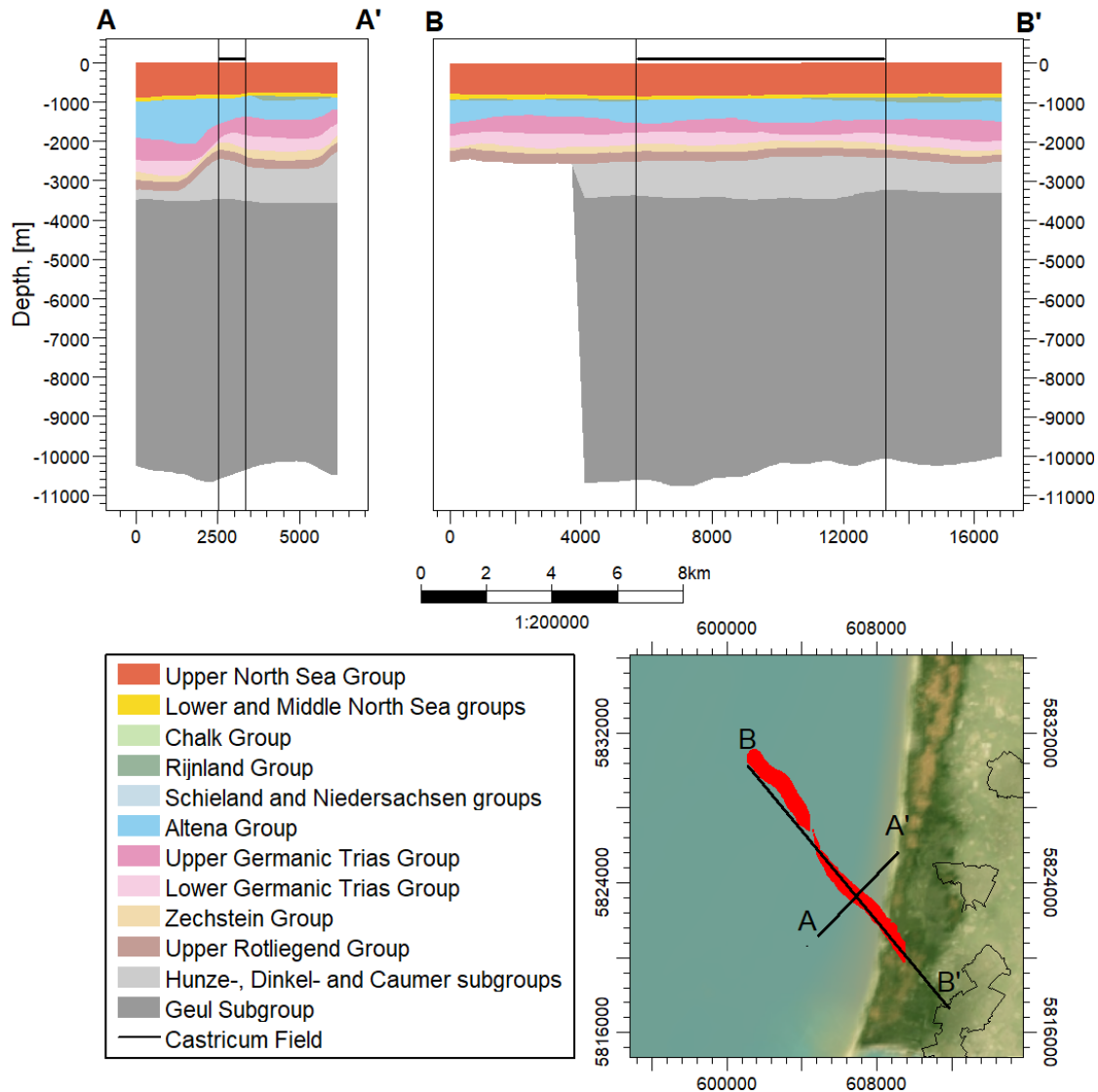


Figure 5. Cross sections and location of the Castricum field showing unconformities across the gas field.

Geological setting Icelandic case study:

Iceland is geologically one of the youngest and most active countries in Europe. Active volcanos, erupting geysers, countless waterfalls, looming glaciers, and tectonic features make the country a paradise for tourists and scientists alike. The island is located in the North Atlantic and is forged by the interaction of excessive volcanic activity and plate spreading. The excessive volcanism is due to a mantle plume situated underneath the island and the spreading is the manifestation of the Mid Atlantic Ridge, a divergent plate boundary which runs along the Atlantic Ocean sea floor. The Mid Atlantic Ridge separates the North America and Eurasia plates, and Iceland is the only place in the world where a spreading ridge rises above sea level. This makes Iceland a unique spot



to study active plate divergence. Geological features on the surface of Iceland are heavily influenced by the plate spreading. The volcanic zones which run through the center of the island from southwest to northeast along the plate boundary are the most active areas on the island, both volcanically and tectonically. On average, we have an eruption every 4-5 years and felt earthquakes multiple times a year. Within the volcanic zones we find the youngest rock formations. They are predominantly basalts. The oldest rock formation onshore are found in the West- and Eastfjords, 16-17 million years old.

The plate boundary that crosses Iceland is offset to the east from the Mid-Atlantic Ridge, towards the Iceland plume. This results in an unstable plate boundary with reoccurring rift transfers in the geological history (Einarsson, 2008; Sigmundsson et al., 2018). These plate boundary offsets are accommodated by transform zones that manifest as highly oblique rift systems and seismic zones, such as the Reykjanes Oblique Rift, the South Iceland Seismic Zone, and the Tjörnes Fracture Zone. According to the NUVEL-1A plate velocity model (DeMets et al., 2010) the velocity of plate spreading in Iceland is on average 18-19mm/yr and the plate velocity direction is N105°E. Most of the spreading is taken up by diking events and normal and strike slip faulting in the volcanic zones.

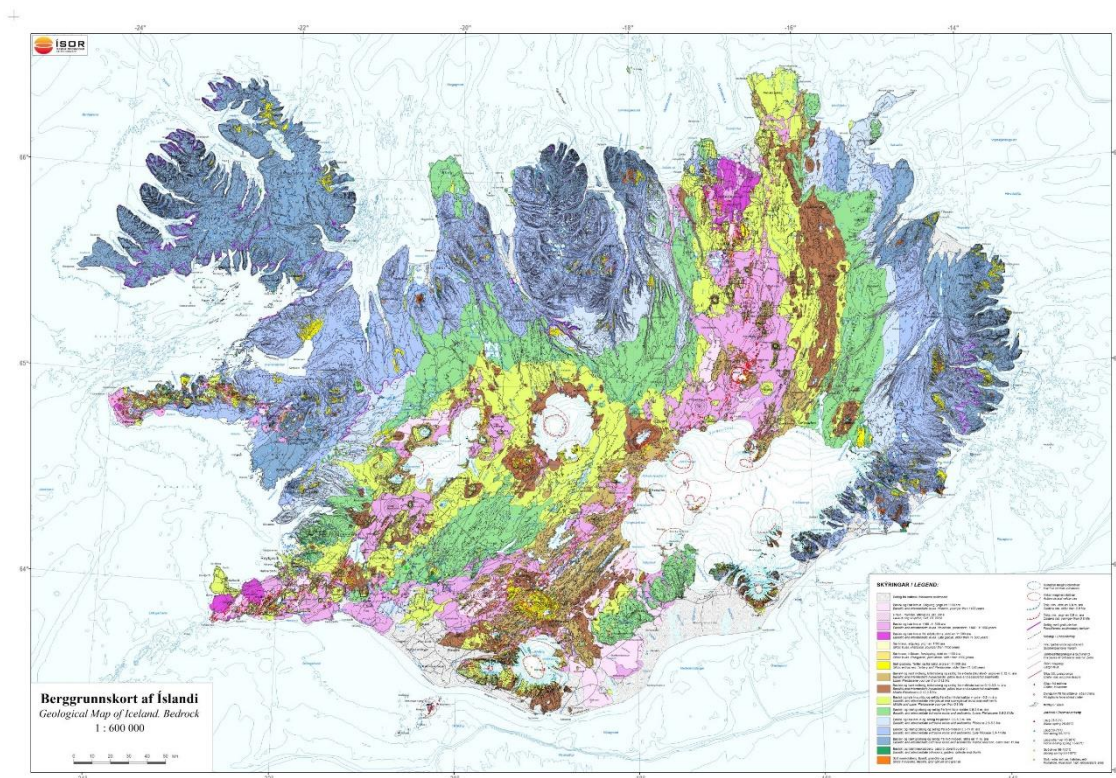


Figure 6 Geological map of Iceland. The map illustrates the main features of the bedrock geology. Formations are colored by age, type, and composition. Older rock formations in the east and west have blue colors while the younger volcanic zones have pink, yellow, and brownish colors (Hjartarson and Sæmundsson, 2014).



7 CASE STUDY ENERGY EXPLOITATION/STORAGE

The case study areas in Iceland, the Netherlands and Denmark cover three different aspects of subsurface utilization: a geothermal field in Iceland, a decommissioned gas field in the Netherlands and active HC producing fields in Denmark.

The case study area in Iceland is on land and equipped with a denser network of seismometers than the offshore case study areas in the Netherlands and Denmark. The selected site contains the Hverahlid Field used for geothermal energy production at the Hellisheidi power plant.

For The Netherlands, we have chosen two decommissioned gas fields as case studies where seismicity occurred after the end of production: the Roswinkel and Castricum gas fields. With new initiatives to re-use old decommissioned gas fields to energy or CO₂ storage together with the fact that seismicity is still occurring at one of the decommissioned gas fields, the exact location and event uncertainty of the seismic events is of high importance. Due to the poor coverage of the seismic network configuration covering the Roswinkel events (seismic national network was upgraded in 2012 by KNMI), we focused on the events of Castricum.

Similarly, in Denmark structures in the North Sea are under consideration as future storage sites for CO₂. This includes both the Nini West depleted reservoir as well as the Hanstholm formation, which is unrelated to hydro-carbon production. Nini West is located far off-shore posing a challenge for land-based earthquake detection. The Hanstholm formation is close to the coast of Jutland, but also close to a known active seismic zone. Improving the quality of hypocentre solutions will add significant value to the process of maturing these reservoirs for future storage. Due to the sparsity of the seismic network and the relatively small number of earthquakes, the whole Denmark is included in the analysis, and not only the oil and gas producing fields in the North Sea.



8 METHODOLOGY

Determining the hypocenter of an earthquake has come a long way since the early days of seismology when seismograms were on paper and basic velocity models were still under construction (e.g., Lehmann, 1987). Today earthquakes are located on a daily basis at national and international data centers, where simple and fast methods such as HYPO-71 (Lee & Lahr, 1972) and derivatives thereof are still in use. These methods use 1D velocity models, and the earthquakes are located at global, regional and national scales. While the analysis is fast, it also carries large uncertainties on the hypocenters, especially in depth. Often the uncertainties are too large to allow the pairing of an earthquake with a specific fault, especially for smaller earthquakes.

Seismicity related to subsurface exploration or storage carries important information about the current state of stress and level of exceedance of fracture strength. Should a fault be reactivated by subsurface activities, well-located microseismicity can illuminate the fault and possibly serve as a first warning that larger events may follow. In other words, reducing uncertainty on earthquake hypocenters is an important factor for mitigating the potential hazard from anthropogenic earthquakes.

Locating earthquakes at reservoir scale requires a local network of seismographs and/or more refined methods depending on the magnitude of events of interest and the level of background noise. In the ideal case the seismographs are evenly distributed around the epicenter. This is seldom the case in real world situations. On land azimuthal gaps in the station coverage can be caused by topography, infrastructure, landowner issues, etc. Obtaining a good azimuthal coverage is even more challenging offshore. Typically, the seismographs recording offshore earthquakes are located on land, resulting in a one-sided and distant coverage.

The challenge of offshore seismograph coverage can be overcome by deploying Ocean Bottom Seismometers (OBS) on the seabed. OBS'es can record excellent data, but they are expensive to use and come with a number of technical challenges. First of all, it is not feasible to have a real-time data connection, and data are collected only once or twice a year. It is therefore hard to use an OBS network as part of a real-time mitigation strategy. Furthermore, the clock on the instruments is not synchronized with GPS or other reliable clocks during deployment, and the absolute time stamps on the data are drifting. Instead of using P- and S-wave arrival times, the analysis is limited to the use of differential P-S time.

In the near future Distributed Acoustic Sensing (DAS) technology is expected to become sufficiently mature for recording earthquakes offshore (e.g., Grandi et al, 2017). This technology carries the potential to significantly improve data density as well as overcoming the real-time challenge for sea bottom installations.

Detailed information on the subsurface velocity structure is also a strong element for reducing uncertainties on the hypocenters. Incorporating this information in earthquake locating programs can be achieved in several different ways.

Applying station corrections to a 1D or 2D velocity model is a simple, but effective way to obtain a pseudo 3D velocity model. Station corrections can be obtained from the analysis of Ground Truth (GT) events. GT events are large explosions where time and



location are known with high precision. In some cases, particularly well-located earthquakes can also serve as GT events. These events are analyzed for systematic deviations in arrival times compared to the expected arrival time at each seismograph for a given velocity model. The resulting station corrections are station specific times that are either added to or subtracted from the observed arrival times. This pseudo 3D method is computationally efficient as the added complexity can be handled by simple lookup tables.

The available software for locating earthquakes with a realistic 3D velocity model is very limited. In this study we have explored a non-linear, probabilistic approach for locating earthquakes in Iceland, the Netherlands and Denmark using the software package NonLinLoc (NLLoc) by Anthony Lomax (Lomax et al., 2000).

NLLoc earthquake location is based on the principles described in Tarantola and Valette (1982), Moser, van Eck and Nolet (1992) and Wittlinger et al. (1993). The Monte Carlo based approach produces in addition to a hypocenter also misfit function, posterior probability density function, and other probabilistic parameters useful for assessing the quality of the hypocenter. The program allows for several different grid search methods. We have chosen to use the Oct-Tree sampling procedure which provides a good balance between search efficiency and completeness. For more details see the NLLoc manual at <http://alomax.free.fr/nlloc/>

Another advantage of NLLoc is the capability to use both simple 1D velocity models with and without station corrections as well as full 3D velocity models. To keep computational costs down, the velocity model is stored as travel-time grid files set up once and for all. This approach makes it equally fast to locate earthquakes using simple and complex velocity models.

The main disadvantage of using NLLoc is that the program is complicated and requires rigorous testing of numerous parameters. The learning curve is steep, and to facilitate the process ISOR wrote up a step-by-step guide to get started in NLLoc (see Chapter 16: Supplementary material) The guide is meant for new users of NLLoc to overcome parts of the challenges of using the software. One of the first steps in setting up the program is to define the velocity grid for the model. The grid must be constructed to include both the expected hypocenters as well as the entire station network. Setting up the velocity grid is trivial for a simple velocity model. However, converting an existing 3D velocity model into a format acceptable by NLLoc is a major challenge. Using the well-known Dutch subsurface and past efforts to estimate 3D velocity models from well data, we used such models as an input to NLLoc. The conversion from the Dutch 3D velocity models to NLLoc was achieved, which can become a future tool for other places in the Netherlands.

Furthermore, the program is very sensitive to the choice of grids. The grid chosen for the solution must be different from the grid defined for the velocity model. The grid used for searching for the hypocenter solution must of course be contained within the velocity grid, and grid boundaries must not coincide. However, the solutions appear to be sensitive to the choice of grids and grid origin, at least for the tests carried out here. This needs to be explored further.



The demand for 3D velocity model based earthquake location is growing with the increased focus on anthropogenic earthquakes in relation to subsurface energy projects such as geothermal energy and CCS. NLLoc has been added as a feature to the widely used and freely available SEISAN earthquake analysis package, Havskov et al 2020, latest version at <http://seisan.info/> NLLoc is born with the ability to read the SEISAN phase file format (S-files), and including NLLoc as an option in SEISAN will provide seismologists across the globe with easy access to an advanced hypocenter location tool. The Seiscomp software also offers the option of locating earthquakes using the NLLoc method (seiscomp.de).

In the case where we introduced a 3D velocity model into NLLoc, the results were still not optimal. To understand the underlying reason, we tested a method based on forward modelling of hyperbolas and their joint likelihood [Milne, 1886], also implemented within NLLoc. The goal was to understand the effect of network configuration and velocity model errors on the estimation of previous epicenter location. Furthermore, the method can help to better select the NLLoc parameters and understand if the poor network configuration of the case-studies of the Netherlands can be an issue even when a 3D velocity model is available. The method assumes single P-phase arrivals at each station.

Finally, another important aspect of monitoring microseismicity and reactivation of dormant faults is to have a highly sensitive and accurate automatic detection and location system. Many different methods exist to achieve this goal but all of them rely on tweaking and tuning several parameters to optimize the sensitivity of the network and the reliability of its locations. ISOR has been working on using machine learning methods to train their Seiscomp system to correctly determine whether a detected event is truly an earthquake or just noise.



9 ANALYSIS, DISCUSSION AND UNCERTAINTY EVALUATION

Results from Denmark

Test of OBS data:

Earthquakes in the Danish part of the North Sea are normally recorded only by the seismograph networks on land. Due to the size and location of Denmark, data from the surrounding countries are included. Still the earthquake catalogue is probably not complete for earthquakes smaller than 2.5 ML (Voss et al., 2015, Larsen et al., 2021). It is therefore worthwhile to explore if deployment of OBSs can provide any significant added value.

The DanSeis experiment (DanSeis infrastructure installation project Southern Scandinavia, 2019) deployed 6 new OBSs in Skagerrak between northern Denmark and southern Norway during the period 2017-Day320 to 2018-Day197. The initial plan was to deploy the instruments in the North Sea, but issues with heavy trawling by fishermen posing a threat to the instruments, could not be resolved in time. The instruments were therefore deployed in Skagerrak instead. During deployment five earthquakes in or close to the North Sea were recorded. Three of the earthquakes were recorded with a high Signal to Noise (S/N) ratio, the last two with weaker signals.

Date	Time, UTC	Lat, deg N	Lon, deg E	Magnitude, ML	Quality
2017 12 08	14:30	56.999	7.192	2.9	Good
2018 01 21	04:29	57.571	7.285	1.7	Good
2018 02 24	09:18	57.303	7.751	1.6	Good
2018 04 16	11:29	57.198	9.091	2.1	Poor
2018 04 17	00:24	57.090	7.817	1.6	Poor

Earthquakes under or close to the North Sea recorded by both the networks of seismographs on land and Ocean Bottom Seismometers.

The OBSs are closer to the epicenter than the land seismographs, although not significantly closer than 100 km. They also narrow one of the larger azimuthal gaps in the station coverage. The noise level at the time of the earthquakes is low, resulting in very sharp signals. However, as the OBSs are without clock synchronization during deployment, the absolute P- and S-wave arrival times cannot be used. Instead the differential P-S time is used. Integrating the OBS-data with the land seismographs still gives slightly higher RMS-errors than when leaving them out. This is likely due to imprecise OBS positions, but needs to be investigated further. Waveforms and epicenter for the 2017-12-08 earthquake are shown in Figure 7.

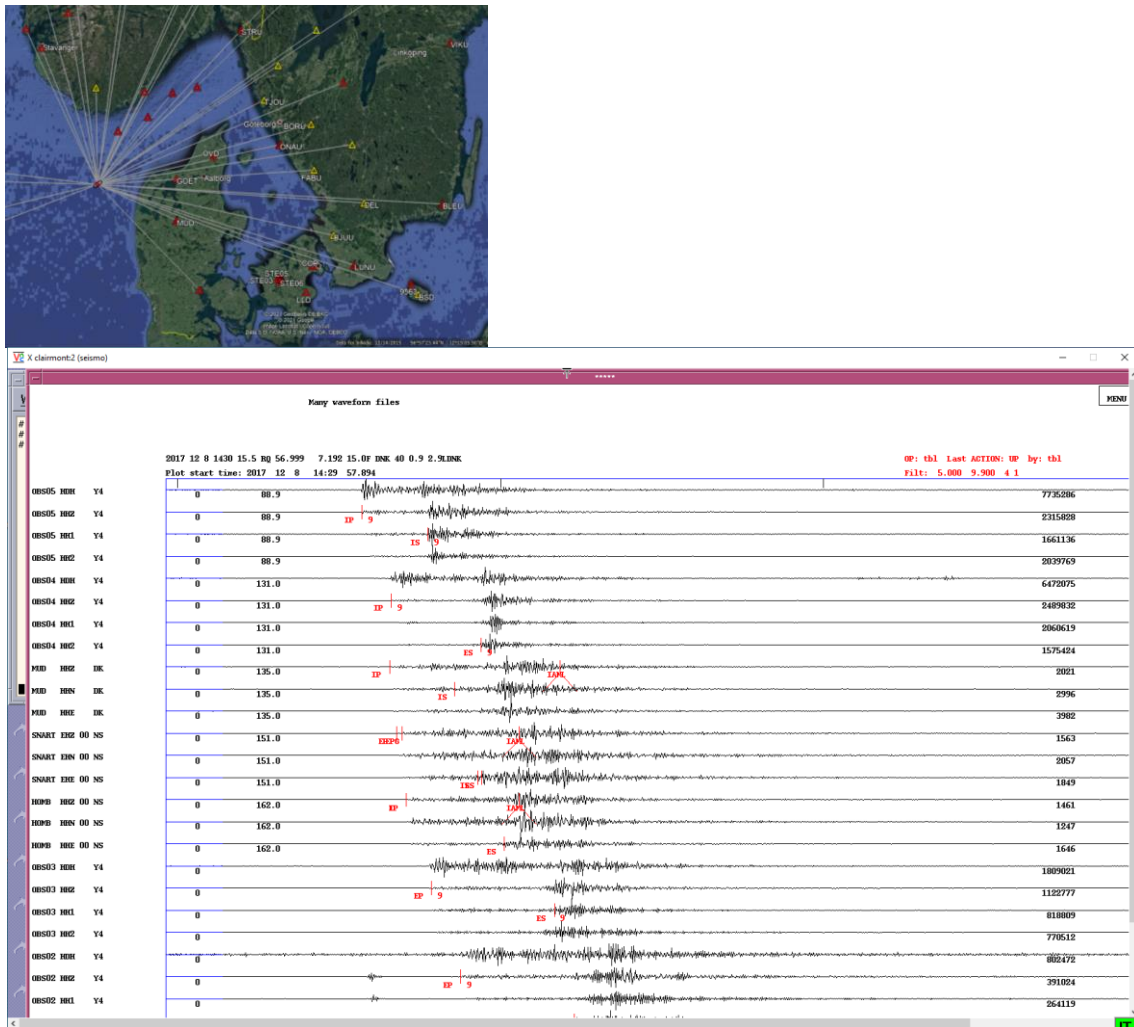


Figure 7: (Top) Earthquake 2017-12-08 epicenter and recording stations, including OBSs. (Bottom) Seismograms from the closest OBSs and land seismographs

Testing NLLoc:

Two well-located Danish earthquakes was chosen for testing NLLoc. This idea was to compare the hypocenter solutions obtained by various configurations of NLLoc with the official GEUS solutions for SEISAN. The selected events are an event in Skagerrak in 2010 and an event in western Jutland in 2018.

Date	Time, UTC	Lat, deg N	Lon, deg E	Magnitude, ML
2010 02 19	21:09	56.875	7.580	3.9
2010 09 16	08:57	56.421	8.189	3.6

The starting point for this investigation was to transform the Danish 1D velocity model to a 3D grid for NLLoc. The idea was to compare the solution obtained by NLLoc to the one from SEISAN using the same velocity model. In this way it would be simple to discern differences in the solution caused solely by differences in method.



Running NLLoc was problematic. When the solution grid was set to cover all of Denmark, and the grid origin was placed in the center of the country, especially longitude appeared poorly constrained. Better results were obtained when the grid origin was placed near the GEUS epicenter, but then the added value in using NLLoc is questionable. Choosing the correct gridding is a well-known issue with NLLoc (e.g., Theunissen et al., 2017) and some more work is required to resolve it beyond this study.

A published 3D velocity model does not exist for Denmark, but unpublished data exists. Once the issues with the solution grid has been resolved and stable results are obtained for the simple velocity model, the realistic 3D velocity model will be implemented.

Results from the Netherlands

The Castricum events

The seismic waveforms can be downloaded from the KNMI website, but we use the phase pickings performed and kindly provided by KNMI and extracted from the corresponding waveforms. We used the picks performed by KNMI of earthquake arrival and assumed an error of 1s for each event pick.

Date	Time, UTC	X in RD [m]	Y in RD [m]	Magnitude
20131023	17:45	100595.476	507824.840	1.9
20131027	08:54	98114.221	508317.005	1.8
20131105	16:51	97106.694	509144.467	1.7
20131128	19:02	98127.339	509448.563	1.7
20131128	20:24	98241.201	509520.689	1.4

Earthquakes located by KNMI

For the determination of the hypocentre locations and corresponding uncertainties, we use the NonLinLoc software (Lomax et al., 2000). The background algorithms of the software use a non-linear global search which then follows a probabilistic inversion formulation. For the network configuration on the estimation of previous epicenter location, we tested a method based on forward modelling of hyperbolas and their joint likelihood [Milne, 1886]. The method assumes single P-phase arrivals at each station and was used in Kamer & Hiemer (2015).

Within the adopted methodology, we investigate three essential aspects concerning an improved event location:

1. Change in the velocity model from 1D to 3D for reducing the error ellipses of uncertainty in earthquake location.
2. Representation of the event uncertainties due to network configuration.
3. Event locations with the most updated HIKE fault database.

1. 1D and 3D velocity model tests

We have collected a 3D P and S-velocity models for the Netherlands available through <https://www.nlog.nl/velmod-31> for each Area of Interest (AOI) as shown in Figure 8. The 3D velocity model was obtained through the information from 1642 boreholes and 3475

velocity data sources (3S or 2D active seismic profiles) [TNO report Pluymaekers, 2017]. The integration of all these data into a 3D velocity model also took into account:

- Sonic logs (all flavours: slowness, instantaneous sonic velocity and calibrated travelttime-depth pairs)
- Check shots / VSP surveys
- TZ curves
- Stratigraphic interpretation of the central stratigraphic units (<https://www.dinoloket.nl/en>)
- Borehole deviation surveys

We prepared all the corresponding phase files and transformation of the available 3D velocity model to a model that can serve as input for NonLinLoc software. For this, we wrote a python script to perform the transformation which will be made available for any future use for event relocation in the Netherlands.

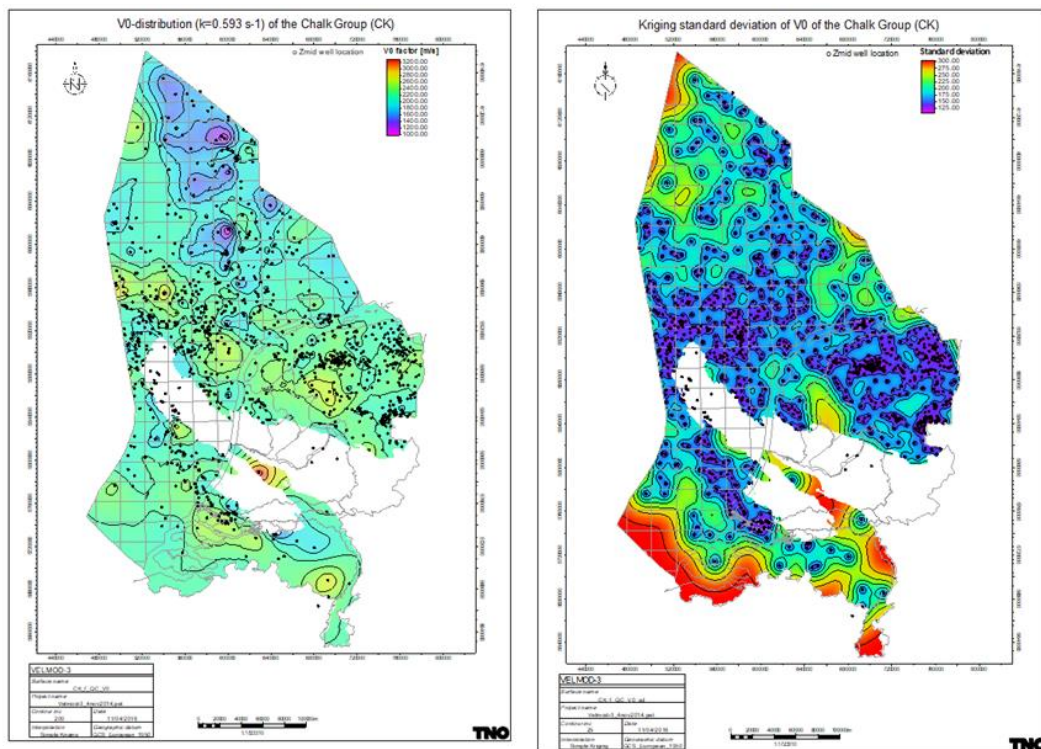


Figure 8 – Example of the velocity distribution of the Chalk group (left) and standard deviation of the corresponding model (right). Adapted from <https://www.nlog.nl/velmod-31>

We tried to estimate first the event location using a 1D velocity model to be able to compare with the KNMI locations and then apply the 3D velocity model. The results of NLLoc for both models were rather disappointing suggesting that or the NLLoc parameters selected were not optimal or that the seismic network configuration was introducing additional uncertainties. The later is mostly because of the squewed network configuration of the stations that were able to capture the events.



2. Event location uncertainty due to seismic network

To allow the estimation of the errors associated with the network configuration only, we assumed that the true P-wave velocity is known, and therefore exactly the same as the modelled P-wave velocity. Additionally, we use 1s (1 standard deviation) as the P-pick uncertainty in an 100m grid resolution.

In Figure 9 we show the application of the method for the Castricum event location and seismic network. The figure shows the used parabolas as well as the resulting spatial Probability Distribution Functions (PDF) of the epicenter and error PDFs of the estimated magnitude, horizontal and vertical coordinates.

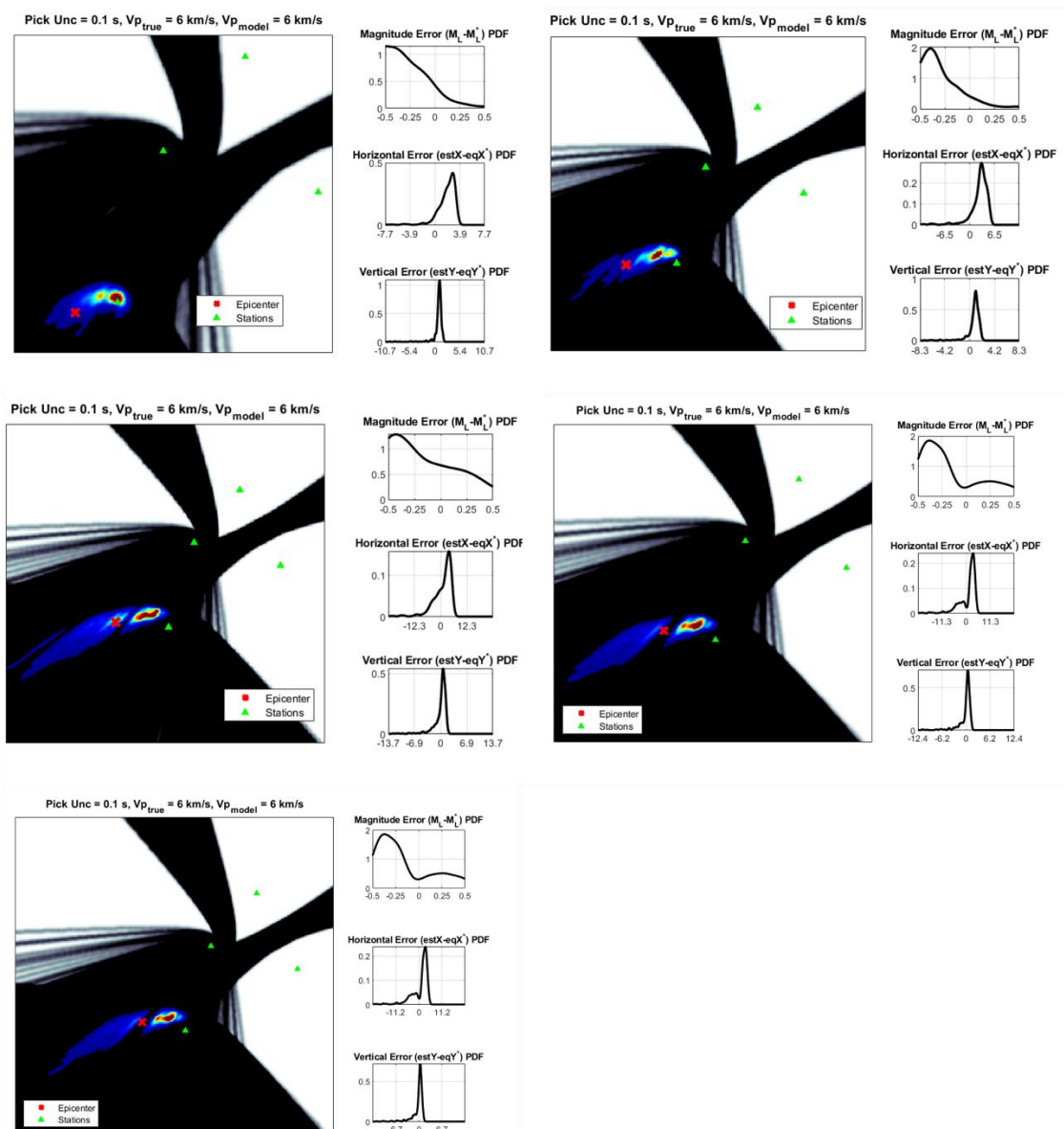


Figure 9. Parabolas and PDF's of the epicenter and error PDFs of the estimated magnitude, horizontal and vertical coordinates for the five events at Castricum.



The results show that the network configuration is not able to reproduce the location of the events (assumed to be the true location) at the highest probability location. In some cases the event location is even outside the estimated error areas. As expected, the vertical and horizontal errors are high when the event is located south of the network configuration for this specific configuration (e.g. the top left Figure 9).

Furthermore, the method can help to select NLLoc parameters and understand if the poor network configuration of the case-studies of the Netherlands can be an issue even when a 3D velocity model is available.

3. Event locations with the most updated HIKE fault database.

Even though the relocation of the Castricum events was not improved because of the above mentioned reasons, the mostly updated HIKE fault database shown that the minimum distance between the previously mapped faults and the estimated event locations is reduced (Figure 10).

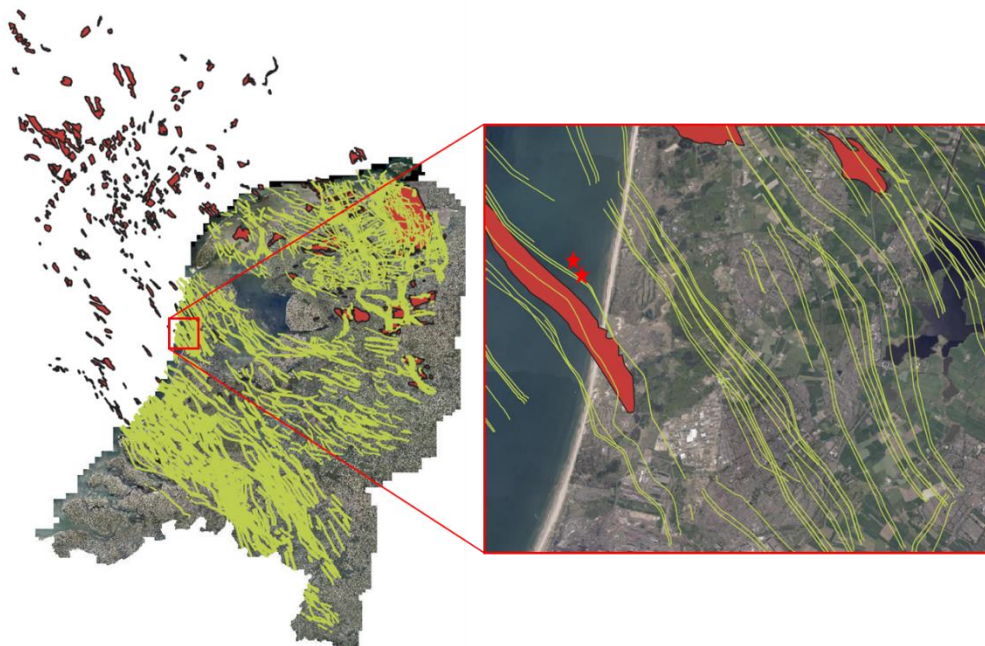


Figure 10– Map of the Netherlands with the newly mapped HIKE faults (yellow lines) and gas fields (red polygons). Zoom figure of the Castricum site with the 1D event relocation.

Results from Iceland

1D velocity model and station corrections

The Hellisheidi power plant in SW Iceland utilises geothermal fields in the Hengill area to produce electricity and hot water for house heating. One of the fields in production is Hverahlid. We used data from 47 temporary and regional seismic networks to develop a new 1D velocity model for the Hverahlid field. We found that two elements were crucial for successful use of the 1D velocity model: station corrections and using a gradient velocity model. The station corrections give individual corrections for the arrival time on each seismic station. This accounts for the difference in the un-accurate 1D model from the real 3D earth. Figure 11 shows the difference between the earthquake locations



when using the 1D velocity model with and without station corrections. The locations with the station corrections is much denser, both in horizontal and vertical location. We also found that the location error was reduced by an order of magnitude.

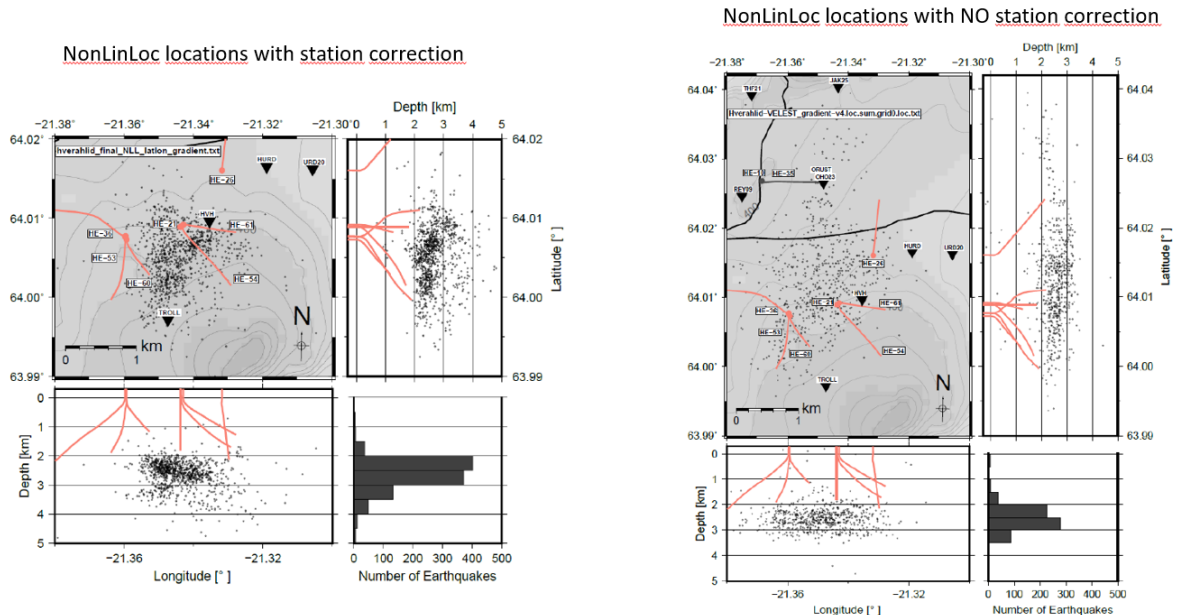


Figure 11 Difference between earthquake locations with and without stations corrections.

The new 1D velocity model is a significant improvement over the older velocity model. In August 2019 shots were exploded in shallow drill holes in Hverahlid. We picked the events and located them in NonLinLoc with the two velocity models. The difference is striking. Figure 12 shows the comparison between the actual locations of the shot holes (stars) and the calculated locations using NonLinLoc (circles). The locations with the new velocity model are significantly closer to the true location of the shot.

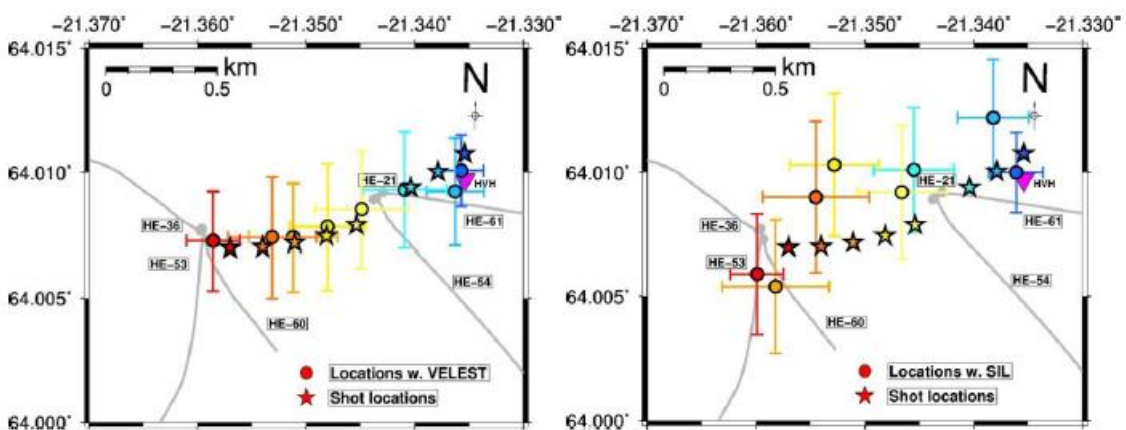


Figure 12 Comparison of the shot hole locations with the locations calculated by picking the arrivals in SeisComP and locating them in NonLinLoc using different velocity models. Crosses show error margins. On the left are locations with the new velocity model. On the right are locations with the older velocity model.



Example of trying to connect seismicity with mapped surface faults

The geothermal field in Hverahlid is an extensively studied area. In an effort to connect the seismicity with mapped surface faults, we calculated relative relocations for several swarms which took place in Hverahlid during the study period. The earthquakes in the seismic swarms are shown on Figure 13. The swarms that clearly delineate a fault have either a N-S strike or N-S striking lineaments on an ENE-WSW striking weak zone. We find a fairly good correlation with mapped surface faults and the faults outlined by seismic swarms.

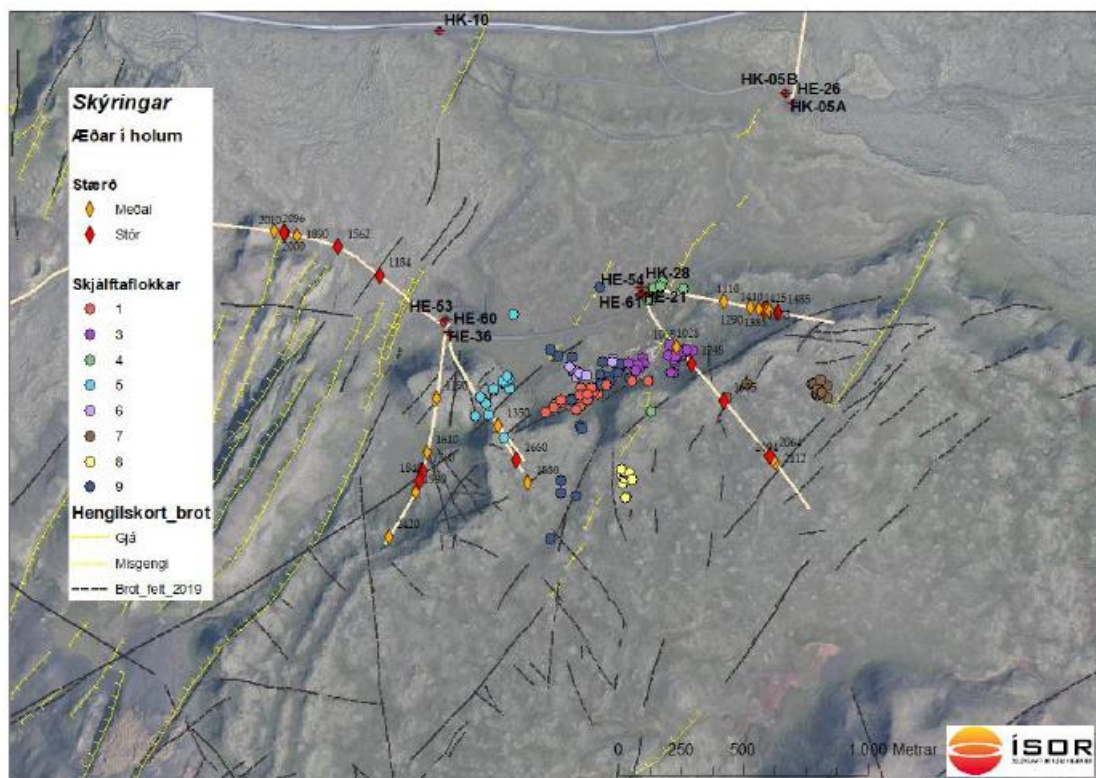


Figure 13 Relative relocations of earthquake swarms in Hverahlid. Also plotted are mapped surface faults from Gunnarsdóttir et al., 2020 in black and from Sæmundsson et al. (2016) in yellow. Well trajectories are in light yellow, and average to large permeable zones in wells displayed with yellow and red diamonds, respectively. The earthquake swarms are coloured with different colours.

Automatic locations and importance for monitoring

Reliable earthquake locations are important for monitoring both natural and induced seismicity. ISOR has a monitoring role of the geothermal fields for two geothermal power companies. To be able to do our job efficiently we want to have a reliable automatic system. One part is to have high quality automatic earthquake locations and the other is to have a system which can easily discern between real seismic events and false detections. A close cooperation between a talented programmer and experienced seismologists has proved most fruitful in this challenge. We have both increased the location accuracy of the automatic system as well as reduced the time needed to review the events manually.



Automatic earthquake monitoring gives event solutions of varying quality in an attempt to correctly locate seismic events. Inevitably, some of these solutions will not be describing real events but are a result of noise. Phase picks on noisy waveforms or wrongly associated phase picks can form a solution that passes the locator's quality threshold that nonetheless does not represent a real earthquake. These can be referred to as false events.

These false events clutter the automatic catalogue and can give a wrong interpretation of seismicity in the monitoring area. This can be fixed with manual review, but if there are many fake events it can take considerable time to manually sort them. Therefore, an automatic solution is preferred. An extra processing step to classify the solutions into 'real event' and 'noise event' can improve the quality of the automatic catalogue drastically. The higher the quality of this classifier is, the higher the confidence in the automatic catalogue is.

While various solutions to this problem are in use today, we found them to be lacking for our area of interest: microseismicity. We wanted to try a machine learning approach to create a classifier which could do better job of sorting incoming detections into real and false events. The classifier uses the relationships between different features of the events to do its job. Ideally the classifier should be good enough so that a human needs never review an event marked as a noise event. Using a Random Forest model with a few well selected features we were able to improve our automatic sorting of events considerably, thereby cutting down on manual review time. The features evaluated by the classifier are properties intrinsic to the event solution such as phase count, RMS error and phase residuals



10 POTENTIAL IMPACT

Reducing uncertainties on hypocenter determination is important for mitigating purposes. Applying pressure changes to the subsurface for e.g. harvesting geothermal energy or storing CO₂ can lead to unintended seismic activity. Being able to track the microseismicity more precisely can serve as a first warning of fault reactivation, thus protecting public safety and infrastructure. Furthermore, precise tracking of microseismicity may allow for quick action if there is increased risk of CO₂ escape in the case of CCS.

Knowing the magnitude of the uncertainties on the hypocenter solutions is equally important. Hypocenters are traditionally presented as dots on a map without further information. However, knowing the extend of the ellipse of uncertainty is critical for the interpretation of the seismicity.

Precise relocation of seismic events can also help to interpret the origin of the events, especially in places where gas/geothermal/other fields overlap or are close to each other. Whereas the triggering mechanism is due to time-dependent effects of compaction due to depletion (differential compaction at the margins of the fields), fluid losses, or friction reduction due to delayed aquifer responses, also require good event relocation as well as uncertainty assessment.



11 IMPORTANCE OF FAULT DATABASE TO IMPROVED HYPOCENTER DETERMINATION METHODOLOGY

Faults are an important factor when assessing subsurface stability. Large fault systems as well as smaller individual faults constitute zones of weakness with the potential to serve as escape pathways for fluids and gasses (see report on Polish case study, D3.4) as well as origins for nucleating sudden energy release in the form of earthquakes. Mapping faults in an area prior to the onset of subsurface projects is a core component of any hazard evaluation. Having a well-documented user-friendly fault database is a good starting point for any subsurface project.

Earthquakes are released in the subsurface when the local stresses exceed the material strength. Earthquakes mainly occur on faults, but small earthquakes can also origin at local weaknesses that are not necessarily fault related, e.g. fluid losses or other operational procedures. Furthermore, not all faults are seismically active. Whether a fault is active or not is important knowledge for the hazard assessment. Various InSAR methods are useful for determining if faults with surface manifestation are mobile (see report on Italian case studies, D3.3), or prone to be reactivated. Seismicity, on the other hand, is the most effective tool to understand possible reasons for a fault to slip. However, connecting faults and earthquake hypocenters is not trivial.

Using standard earthquake analysis tools and the commonly available data often results in hypocenters with uncertainties too large to connect a specific earthquake to a specific fault. The seismicity mapped in this manner is useful for determining the general seismic hazard in the area, but it is insufficient to discern if a given fault is active or not.

Reducing the uncertainty on the hypocenters can lead to better distinction between active and passive faults. In connection with subsurface projects such as CCS it is critical to know if a fault inside or close to a reservoir is active or not.

During the implementation of subsurface storage or exploitation of oil, gas or hot water/steam, the pressure changes caused by injection or extraction may cause seismicity. Microseismicity occurring close to the well is not necessarily a cause of concern. However, if the earthquakes begin to light up along a fault, this should be taken as a sign of warning. Reactivation of a fault is considered a high-risk situation with the potential for larger earthquakes to occur as seen in Oklahoma (Keranen et al., 2014). Even without large earthquakes or significant damages, a reactivated fault can be a showstopper for subsurface projects as seen at the CO₂ storage project in In Salah, Algeria (e.g. Goertz-Allmann et al., 2014, Rinaldi and Rutqvist, 2013), the EGS system in Basel, Switzerland (Deichmann and Giardini, 2009) and possibly jeopardise subsurface exploitation. .

A high quality fault database as well as precise hypocenter determination is crucial for detecting the first signs of instability as expressed in small induced earthquakes.. A detailed Fault Database playing in concert precise hypocenter determination is a critical pillar in safe storage and exploitation. Together this can form the basis for efficient mitigation such as the Traffic Light System (TLS).



12 CROSS-CUTTING RELATIONS BETWEEN CASE STUDIES

The case studies apply different methodologies to the study of the potential hazards and impacts across several different kinds of energy exploitation. There are different varieties of exploitation being studied using the same methodologies, and the potential hazards and impacts for similar types of energy exploitation are being investigated using different methodologies. The following settings are investigated: a geothermal field (T3.1), decommissioned gas fields ((T3.1, T.3.4), active gas fields (T3.1, T.3.2), active oil fields (T3.1, T.3.3), and decommissioned CO₂ -storage (T.3.4). The applied technologies are seismology (T3.1, T3.4), InSAR-based methods (T3.2), and fault seal analysis (T3.3). All case studies have at least one cross-cutting methodology and/or exploitation type relation to another.

In addition to the energy exploitation type/hazard methodology cross-cutting relations, two overarching common themes have been explored: 1) How the different methodologies deal with uncertainties in different situation, and 2) how to improve the input to guidelines made by authorities.

12.1 Cross-cutting: uncertainty estimates

The methodologies being studied have different ways to deal with uncertainties, and different technologies produce uncertainties on very different spatial scales. Where surface displacement can be measured with mm precision using various InSAR-based methods, seismology works with uncertainties on epicenters of hundreds of meters and for sparse data sets of km scale. A common cross-cutting theme is: Do the uncertainties permit us to relate a specific fault to a potential hazard? In some cases inherent differences exist between the different types of data and models we would like to relate.

T3.1, Advanced localization of seismicity,

Quantifying uncertainty on hypocenters is important for relating specific events to specific faults. The extend of a fault is known with much greater precision than is obtainable for seismic events. When assessing potential hazards related to a fault, it is therefore useful to know if the fault is within the error ellipse of the hypocenter solution, as the hypocenters will typically be more scattered.

Discerning between natural seismicity and anthropogenic seismicity can be difficult. A small uncertainty ellipse on the hypocenters can help discriminating with more certainty, especially if the events cluster or line up in geologically distinct areas.

12.2 Cross-cutting: Scientific basis for further operations

A common, cross-cutting goal for all of the case studies is the desire to provide improved scientific input to the assessment of hazard for further studies or for authorities writing guidelines for the safe storage and energy exploitation of the subsurface. Without proper attention and precautions, activities may lead to unwanted side effects such as earthquakes, subsidence and leakage. Guidelines based on the latest scientific findings and recognizable standards can contribute to improved safety in storage and energy



exploitation. Improved standards may also aid in the communication with the general public where safety is of great interest.

In addition to the evaluation of each potential hazard in the case studies, it is relevant to consider that several different hazards may be relevant for a given energy exploitation project. For the authorities it is important to consider what is the impact of each hazard in a combined multi-hazard assessment. While HIKE may not be able to produce such a formula, the knowledge generated in the project will be made available through the Knowledge Data Base, thus highlighting the different hazards to take into account.



13 BEST PRACTICE WITHIN THE FIELD OF EARTHQUAKE LOCATION AND MONITORING

It is still common practice to use simple and fast methods based on 1D velocity models and the principles from HYPO-71 (Lee & Lahr, 1972). This allows for fast, near-realtime analysis of large numbers of earthquakes, as is required for monitoring at injection projects. Using a simple and fast analysis method makes it possible to include data from a large number of seismographs. This can secure a dense azimuthal coverage as well as cover a wide range of distances. High quality hypocenters can be achieved in this way (e.g., Bondar et al, 2019). Further improvements can be achieved by upgrading the 1D velocity model with station corrections from Ground Truth events as demonstrated in this report.

For study areas with many small events relatively close together, relative location methods such as HypoDD (Waldhauser and Ellsworth, 2000) can be effective. The basis for the location is still a 1D velocity model. A well-located earthquake, typically one of the largest, serves as a master event. Smaller events are then located relative to the master. This is useful for locating induced seismicity where many small events need to be located in a confined area. Cross-correlation is another analysis method where a high-quality master event is used for detecting and locating smaller events (e.g. Goertz-Allmann et al., 2014)

However, the simple methods do typically not provide good statistical information on hypocenter uncertainties. This can be achieved by using Monte Carlo based analysis tools such as NonLinLoc. This class of methods is still not sufficiently user friendly to become widely used, but progress is being made. During the HIKE project a user friendly getting started manual for NonLinLoc has been developed (see Chapter 16: Supplementary Material), and easy access to the program through the seismic analysis package SEISAN has been established.

A different approach for locating earthquakes uses full waveform inversion. This can achieve high quality results but is even more complicated to implement. Waveform inversion is described in the French case study report, D3.5.

No matter the analysis method, the quality of the velocity model appears to be more important than the complexity of the method. A well-constrained 1D velocity model may produce better results than a poorly constrained 3D velocity model (Theunissen et al, 2018). Strong methods and data are at the core of any high-quality earthquake monitoring system. While instrumentation is constantly improving it has become clear from this study that improved velocity models are crucial, and a field that needs more attention. Analytical methods are also improving, but without good velocity models, the fancy methods are not of much use.



14 RELEVANCE OF THIS STUDY TO THE NEW GREEN DEAL AND PROPOSED FUTURE STUDIES

Induced and triggered seismicity can occur in connection with projects involving injection of fluids into the subsurface. The injected fluids change the local stress field which can then lead to microseismicity or even larger earthquakes. High-pressure stimulation under hard rock conditions is known to induce larger earthquakes than soft geology as seen e.g. in connection with the deep geothermal project in Basel (Deichmann and Giardini, 2009).

Geothermal Energy as well as Carbon Capture and Storage (CCS) are candidates as Green Solutions for the future. To harvest geothermal energy, cold water is injected into the subsurface and hot water is retrieved. The process can induce earthquakes and microseismic monitoring is needed.

CCS is a possible solution to rid the atmosphere of excess CO₂. CO₂ can be captured at point sources such as powerplants and injected into the subsurface. If the injection changes the stresses more than the reservoir can accommodate, earthquakes may result.

In order to avoid inducing problematic earthquakes it is important to carry out a proper hazard analysis before initiating an injection project. Such a hazard analysis has two core components: mapping of faults and analyzing natural seismicity in and around the area of interest. The quality of such a hazard analysis is highly dependent on the quality of the input data: A precise mapping of faults combined with earthquake hypocenters with small uncertainties is desirable. It is desirable if the uncertainty on the hypocenters can be reduced sufficiently that the seismicity can be associated with the mapped faults.

Determining the earthquake hypocenters with small uncertainty can also be part of a mitigation system. Monitoring the spatial-temporal evolution of microseismicity around injection wells can reveal if stress changes are exceeding a problematic level. An increase in the number of small earthquakes or an increase in the earthquake magnitudes can be seen as a sign of warning. If realtime monitoring captures such changes it is possible to reduce the injection pressure until the subsurface has adjusted, and the microseismicity has dropped to an acceptable level again.

High quality monitoring of microseismicity is becoming increasingly important with the rise of green injection projects. In addition to the improvement of analysis methods the future will see more advanced observational methods such as fiber optics solutions. The use of fiber optics in seismology is still a young field of research and more work is needed on data collection as well as data processing.

Finally, it is critical to allocate resources to improve velocity models in the area of interest as the hypocenter solutions depend strongly on good knowledge of the medium which the waves propagate through.



15 REFERENCES

Bondar, I., Myers, S., Engdahl, E. & Bergman, E., 2004. Epicentre accuracy based on seismic network criteria, *Geophys. J. Int.*, **156**(3), 483–496.

Buijze, A. J. L. (2020). Numerical and experimental simulation of fault reactivation and earthquake rupture applied to induced seismicity in the Groningen gas field, Utrecht University.

De Jager, J., M. Geluk, T. E. Wong, D. Batjes and J. de Jager (2007). "Geology of the Netherlands." Petroleum Geology. Royal Netherlands Academy of Arts and Sciences, Amsterdam, The Netherlands 241: 264.

Deichmann, N., Giardini, D. 2009. Earthquakes Induced by the Stimulation of an Enhanced Geothermal System below Basel (Switzerland). *Seismol. Res. Lett.* 80:784–798; doi:10.1785/gssrl.80.5.784

Dienst, R. G. (1994). "Geological Atlas of the Subsurface of the Netherlands, explanation to map sheet V." Sneek-Zwolle. Haarlem: 1-126.

Dost, B., Van Eck, T., & Haak, H. (2004). Scaling of peak ground acceleration and peak ground velocity recorded in the Netherlands. *Bollettino di Geofisica Teorica ed Applicata*, 45(3), 153-168.

Duin, E., J. Doornenbal, R. Rijkers, J. Verbeek and T. E. Wong (2006). "Subsurface structure of the Netherlands-results of recent onshore and offshore mapping." *Netherlands Journal of Geosciences* 85(4): 245.

Fokker, P. A., Visser, K., Peters, E., Kunakbayeva, G., & Muntendam-Bos, A. (2012). Inversion of surface subsidence data to quantify reservoir compartmentalization: A field study. *Journal of Petroleum Science and Engineering*, 96, 10-21

Goertz-Allmann, Kühn, D., Oye, V., Bohloli, B., & Aker, E., 2014, Combining microseismic and geomechanical observations to interpret storage integrity at the In Salah CCS site, *Geophys. J. Int.*, Vol. 198, 447-461.

Grandi, S., Dean, M., & Tucker, O., Efficient containment monitoring with distributed acoustic sensing: feasibility studies for the former Peterhead CCS Project, 2017, *Energ. Proc.*, V. 114, 3889-3904.

Gunnarsdóttir, S. H., Kristinsson, S. G. and Nielsson, S. (2020). Hverahlíð – Norðurhálsar. Mið fyrir rannsóknarborholur. Iceland GeoSurvey, Reykjavík, report, ÍSOR-2020/005, 20 p.

Gutenberg, B. and C. F. Richter (1941). "Seismicity of Central and south América." *Geol. Sc* 4: 455.



Havskov, J., Voss, P.H. and Ottemoller, L. (2020). Seismological Observatory Software: 30 Yr of SEISAN. *Seismological Research Letters*, 91 (3): 1846-1852. DOI: <https://doi.org/10.1785/0220190313>

[Hjartarson, Á. and Sæmundsson, K. \(2014\). Geological Map of Iceland. Bedrock. 1:600 000. Iceland GeoSurvey.](#)

Husen, S., E. Kissling, N. Deichmann, S. Wiemer, D. Giardini and M. Baer (2003). "Probabilistic earthquake location in complex three-dimensional velocity models: Application to Switzerland." *Journal of Geophysical Research: Solid Earth* 108(B2).

Kamer, Y. and S. Hiemer (2015). "Data-driven spatial b value estimation with applications to California seismicity: To b or not to b." *Journal of Geophysical Research: Solid Earth* 120(7): 5191-5214.

Keranen, K.M., Weingarten, M., Abers, G.A., Bekins, B.A., & Ge, S., 2014, Sharp increase in central Oklahoma seismicity since 2008 induced by massive wastewater injection, *Science*, doi: 10.1126/science.1255802

Kombrink, H., J. Doornenbal, E. Duin, M. Den Dulk, J. Ten Veen and N. Witmans (2012). "New insights into the geological structure of the Netherlands; results of a detailed mapping project." *Netherlands Journal of Geosciences* 91(4): 419-446.

Larsen, T.B., Voss, P.H., Dahl-Jensen, T., 2020, Seismology in relation to safe storage of CO₂, Geological Survey of Denmark and Greenland report, 2020/41, pp 28.

Lassen, A. & Th ybo, H. 2012: Neoproterozoic and Palaeozoic evolution of SW Scandinavia based on integrated seismic interpretation. *Precambrian Research* 204–205, 75–104.

Lehmann, I. (1987), Seismology in the days of old, *Eos Trans. AGU*, 68(3), 33-35, doi:10.1029/EO068i003p00033-02. *Eos* (Washington, D.C.), 1987-01-20, Vol.68 (3), p.33-35

Lomax, A., A. Zollo, P. Capuano and J. Virieux (2001). "Precise, absolute earthquake location under Somma–Vesuvius volcano using a new three-dimensional velocity model." *Geophysical Journal International* 146(2): 313-331.

Milne, J. (1886). *Earthquakes and other earth movements*, K. Paul, Trench.

Nielsen, L.H., 2003: Late Triassic-Jurassic development of the Danish Basin and Fennoscandian Border Zone, Southern Scandinavia. *Geological Survey of Denmark and Greenland Bulletin* 1, 459-526.

Rinaldi, A.P. & Rutqvist, J. 2013: Modeling of deep fracture zone opening and transient ground surface uplift at KB-502 CO₂ injection well, In Salah, Algeria. *International Journal of Greenhouse Gas Control* 12, 155–167.



Sæmundsson, K., Sigurgeirsson, M. Á., Hjartarson, Á., Kaldal, I., Kristinsson, S. G. and Víkingsson, S. (2016). Geological map of Southwest Iceland, 1:100.000 (2nd edition). Reykjavík, Iceland GeoSurvey.

Theunissen, T., S. Chevrot, M. Sylvander, V. Monteiller, V., M. Calvet, A. Villasenor, S., Benahmed, H. Pauchet, and F. Grimaud, Absolute earthquake locations using 3-D versus 1-D velocity models below a local seismic network: example from the Pyrenees, *Geophys. J. Int.* (2018) **212**, 1806–1828, doi: 10.1093/gji/ggx472

TNO report (2016). Evaluatie mogelijke oorzaak aardbevingen nabij Castricum-Zee in oktober – november 2013. (<https://www.sodm.nl/rapporten>)

Vejbæk, O.V. 1997: Dybe strukturer i danske sedimentære bassiner. *Geologisk Tidsskrift* 4, 31 pp.

Voss, P., Dahl-Jensen, T., and Larsen, T. B., 2015, Earthquake Hazard in Denmark: Geological Survey of Denmark and Greenland report, 2015/24, pp 53.

Waldhauser F. and W.L. Ellsworth, A double-difference earthquake location algorithm: Method and application to the northern Hayward fault, *Bull. Seism. Soc. Am.*, 90, 1353-1368, 2000.

Wilson, M. P., Foulger, G. R., Gluyas, J. G., Davies, R. J., & Julian, B. R. (2017). [HiQuake: The human-induced earthquake database](#). *Seismological Research Letters*, 88(6), 1560-1565.

Wong, T. E., I. De Lugt, G. Kuhlmann and I. Overeem (2007). Tertiary. *Geology of the Netherlands*, Royal Netherlands Academy of Arts and Sciences: 151-171.

<https://www.nlog.nl/velmod-31>
<https://www.dinoloket.nl/en>



16 SUPPLEMENTARY MATERIAL: FIRST STEPS IN NONLINLOC

***Disclaimer:** This guide should help you with your first steps in NonLinLoc. It is compiled by seismologists at ÍSOR and is specific for studying local seismicity. Nevertheless, anyone should be able to use it get started. If you have any comments or suggestions for improving the guide, please contact Sigríður Kristjánsdóttir (Sissa), e-mail: sigridur.kristjansdottir@isor.is.

1.0 Purpose

This file explains how to run the NonLinLoc software and how to prepare the relevant input files. NonLinLoc (Non-Linear Location) is a non-linear location method and is created by Anthony Lomax. Both 1D and 3D velocity models can be used and the height of the seismometer is taken into account. NonLinLoc returns reliable earthquake locations with uncertainties. The following sections describes each step of how to run NonLinLoc successfully.

2.0 Creating a working directory

Create a directory to work in on /export/skjalftagogn/vinnsla. The name of the directory should include the the name of the area that we will be working on and some other identifier if there are other directories for the same area. Examples for directory names: reykjanes-2020, husmuli-2011.

Create a sub-directory for NonLinLoc. It can e.g. be called NLLC.

Create 5 subdirectories in the NLLC directory:

```
loc
model
obs
run
time
```

Put the config file in the run directory. You can copy an old one from previous projects if you have it and modify it.

3.0 Creating phase files for NonLinLoc

Observation files for NonLinLoc can have 8 different formats, and they are all described on the NonLinLoc webpage (<http://alomax.free.fr/nlloc/>). At ISOR we use the NonLinLoc phase file format.

This is an example of the first few lines of a phase file used for Hverahlid earthquakes:

```
BIT06 2C ? ? P D 20181129 0525 42.6536 GAU 2.00e-02 0.00e+00 0.00e+00 0.00e+00 1.00e+00
BJA SI ? ? P U 20181129 0525 42.9056 GAU 2.00e-02 0.00e+00 0.00e+00 0.00e+00 1.00e+00
BLK22 2C ? ? P U 20181129 0525 42.9456 GAU 2.00e-02 0.00e+00 0.00e+00 0.00e+00 1.00e+00
BLK22 2C ? ? S ? 20181129 0525 44.3146 GAU 2.00e-02 0.00e+00 0.00e+00 0.00e+00 1.00e+00
EDA SI ? ? P U 20181129 0525 43.0806 GAU 2.00e-02 0.00e+00 0.00e+00 0.00e+00 1.00e+00
EDA SI ? ? S ? 20181129 0525 44.3896 GAU 2.00e-02 0.00e+00 0.00e+00 0.00e+00 1.00e+00
FAL44 2C ? ? P ? 20181129 0525 43.4806 GAU 2.00e-02 0.00e+00 0.00e+00 0.00e+00 1.00e+00
FAL44 2C ? ? S ? 20181129 0525 45.2936 GAU 2.00e-02 0.00e+00 0.00e+00 0.00e+00 1.00e+00
GAN02 2C ? ? P U 20181129 0525 43.2966 GAU 2.00e-02 0.00e+00 0.00e+00 0.00e+00 1.00e+00
GRAFN ON ? ? P D 20181129 0525 44.0086 GAU 2.00e-02 0.00e+00 0.00e+00 0.00e+00 1.00e+00
GRH43 2C ? ? P U 20181129 0525 42.0716 GAU 2.00e-02 0.00e+00 0.00e+00 0.00e+00 1.00e+00
GRH43 2C ? ? S ? 20181129 0525 42.7186 GAU 2.00e-02 0.00e+00 0.00e+00 0.00e+00 1.00e+00
```

We use bash scripts to create the input files from scbulletins that come out of Seiscomp.



4.0 Create a NonLinLoc control file

The NonLinLoc control file is composed of the following control file statements:

- Generic
- Vel2Grid
- Grid2Time
- NLLoc

Each of these parts is made up of several commands. Each command is described below, but they all share the same control file syntax: a control keyword in upper case letters followed by one or more control parameters, all written on the same line.

Generic control file statements

```
CONTROL 3 54321
```

The first number sets the verbosity level for error messaging which is printed to the terminal.

- -1 = completely silent,
- 0 = error messages only,
- 1 = 0 + higher-level warning and progress messages,
- 2 and higher = 1 + lower-level warning and progress messages + information messages

Our choice, 3, prints out all messages.

The second number is an integer which NonLinLoc uses to generate random number sequences for Metropolis samples and by program Time2EQ to generate noisy time picks. The value 54321 is the default.

```
TRANS SIMPLE 64.05 -21.39 0.0
```

Our value for the transformation is SIMPLE. The SIMPLE transformation only corrects longitudinal distances as a function of latitude and is good enough for a small area like we are usually working with (size ~10/100s of km). This is the algorithm that NonLinLoc uses and is taken from the website:

- $x = (\text{long} - \text{longOrig}) * 111.111 * \cos(\text{lat_radians});$
- $y = (\text{lat} - \text{latOrig}) * 111.111;$
- $\text{lat} = \text{latOrig} + y / 111.111;$
- $\text{long} = \text{longOrig} + x / (111.111 * \cos(\text{lat_radians}))$

The first two numbers after the TRANS SIMPLE command are the center of a grid of the region of interest and are given in latitude (-90.0 to 90.0) and longitude (-180.0 to 180.0). In this example the region of interest is Husmuli in Hengill and the latitude and longitude are the center point of that area. The last number is only used if your area is rotated.

Vel2Grid control file statements

Vel2Grid control file statements create a three dimensional velocity grid from a given velocity model. The grid is saved in header and buffer files. These files contain information about the velocity, slowness or other characteristics of the velocity model.

```
VGOUT ./model/layer.model
```

VGOUT creates velocity grid files (.buf and .hdr files) which will be saved in a sub-directory called model.



VGTYPE P

Tell the program to calculate a velocity grid for P waves. You can only run for either P or S at a time. We do this by commenting out the VGTYPE S line when we are running for the P wave and vice versa.

VGTYPE S

Tell the program to calculate a velocity grid for S waves. You can only run for either P or S at a time. We do this by commenting out the VGTYPE S line when we are running for the P wave and vice versa.

What you have to do is execute the Vel2Grid command once with the VGTYPE S line commented out and then again with the VGTYPE P commented out.

VGGRID 2 2001 921 0.0 0.0 -2.0 0.025 0.025 0.025 SLOW_LEN

2 = number of grid nodes in the x direction, must be 2 for 2D grids

2001 = number of grid nodes in the y direction

921 = number of grid nodes in the z direction

0.0 = x location of the grid origin in km relative to the geographic origin

0.0 = y location of the grid origin in km relative to the geographic origin

-2.0 = z location of the grid origin in km relative to the geographic origin

The geographic origin is given in the TRANS SIMPLE command above.

0.025 = grid node spacing in kilometers along the x axes

0.025 = grid node spacing in kilometers along the y axes

0.025 = grid node spacing in kilometers along the z axes

SLOW_LEN = physical quantity to store on grid, slowness * grid node spacing (sec)

For the values that we have chosen here the size of the grid is (2001-1) * 0.025 km = 50 km in the y direction and (921-1) * 0.025 km = 23 km in the z direction. And it is centered on the coordinates given in TRANS SIMPLE (64.01 -21.35) but the velocity grid starts 2.0 km above sea level (-2.0 km „above“ the 0.0 reference depth). If you are working in a very small area you can have a very fine grid. The area in Hverahlíð which we were working on was only a few kilometers across.

Next up is the velocity model.

LAYER	-2.0	2.500	0.410	1.420	0.2330	0.0	0
LAYER	0.0	3.320	0.880	1.886	0.5000	0.0	0
LAYER	1.0	4.200	0.830	2.386	0.4716	0.0	0
LAYER	2.0	5.030	0.882	2.858	0.5010	0.0	0
LAYER	3.1	6.000	0.156	3.409	0.0884	0.0	0
LAYER	4.0	6.140	0.170	3.489	0.0966	0.0	0
LAYER	5.0	6.310	0.160	3.585	0.0909	0.0	0
LAYER	6.0	6.470	0.156	3.676	0.0884	0.0	0
LAYER	7.8	6.750	0.800	3.835	0.4545	0.0	0
LAYER	8.0	6.910	0.030	3.926	0.0170	0.0	0
LAYER	10.0	6.970	0.024	3.960	0.0136	0.0	0
LAYER	15.0	7.090	0.020	4.028	0.0114	0.0	0
LAYER	20.0	7.190	0.014	4.085	0.0080	0.0	0
LAYER	25.0	7.260	0.000	4.125	0.0000	0.0	0

Each line is like this:

LAYER depth Vp_top Vp_grad Vs_top Vs_grad rho_top rho_grad

We found great improvement in using a gradient velocity model.



Grid2Time control file statements

Grid2Time control file statements calculates the travel times from source points in a three dimensional velocity grid to all other grid points of the grid.

```
GTFILES ./model/layer.model ./time/layer P
GTFILES ./model/layer.model ./time/layer S
```

./model/layer.model = input file root

The path to the input file is defined in the VGOUT command line so it has to be the same here.

./time/layer = output file root

The path to the output file.

P or S = wave type

What you have to do is execute the Grid2Time command once with the GTFILES

./model/layer.model ./time/layer S line commented out and then again with the GTFILES

./model/layer.model ./time/layer P commented out.

```
GTMODE GRID2D ANGLES_YES
```

GRID2D = grid type (two options are available GRID3D and GRID2D, GRID3D for a 3D grid and GRID2D for a 2D grid)

ANGLES_YES = option for calculating the take-off angles an output an angles gird (ANGLES_YES tells the program to calculate the angles and ANGLES_NO tells the program to not calculate the angles).

```
GTSRCE BIT LATLON 64.05730 -21.25770 -0.39 0
GTSRCE BJA LATLON 63.94590 -21.30258 -0.057 0
GTSRCE BLF LATLON 63.97368 -21.64893 -0.548 0
GTSRCE BOLI LATLON 64.06255 -21.41332 -0.259 0
GTSRCE BUG LATLON 63.90450 -21.43760 -0.034 0
GTSRCE ENG LATLON 64.08786 -21.41053 -0.27 0
GTSRCE GEI LATLON 63.94815 -21.53067 -0.339 0
...
```

These lines contain the location of the seismic stations. There are four different syntax options for this command. We use the one for decimal degree of latitude and longitude. Other options are explained on the NonLinLoc website.

Syntax explanation:

GTSRC	STATION_NAM	TYPE_OF_LOCATIO	COORDINATE_1	COORDINATE_2	DEPT	HEIGH
E	E	N	1	2	H	T
GTSRC	TROLL	LATLON	63.9972300	-21.3473800	0	0.4410
E						

The information can also be put in a file with the same format. Then you have to put in one line in the config line instead of the GTSRCE lines. The line is: INCLUDE /home/sysop/nll/data/stations-HE.nll. The line is just INCLUDE followed by the path to the station file.

```
GT_PLFD 1.0e-3 0
```

Selection for Podvin and Lecomte finite difference method and specification for method parameters.



1.0e-3: fraction defining the tolerated model inhomogeneity for exact initialization. A tolerance larger than 0.01 will potentially create errors larger than those involved by the F.D. scheme without any exact initialization. (from the NonLinLoc website).

0: error message flag. 0: silent, 1: few messages, 2: verbose. A negative value inhibits a clever initialization (NonLinLoc website).

Time2EQ control file statements

```
EQFILES ./time/layer ./synth.husmuli_obs
```

Root of the input files with the input time grids generated by Grid2Time and path and name of output phase/observation file. [EQFILES <input file root> <output file>].
The root of the input files has to be the same as the second variable in the GTFILES command line (see above in Grid2Time control file statements section).

```
EQMODE SRCE_TO_STA
```

Tell the software whether to calculate time for a single source to multiple stations or the other way around, calculate time for multiple sources to a single station.

SRCE_TO_STA = calculate time for single source to multiple stations

STA_TO_SRCE = calculate time for multiple sources to a single station

We are calculating locations of earthquakes with respect to all stations, therefore we choose SRCE_TO_STA.

```
EQQUAL2ERR 0.1 0.5 1.0 2.0 99999.9
```

Specifies the mapping of error to phase pick quality for output of phase/observations in HYPO71 file format. HYPO71 doesn't read phase errors only quality.

0.1 0.5 1.0 2.0 99999.9 -> Errors between 0.0 and 0.1 are output with quality 0, errors with output between 0.1 and 0.5 are output with quality 1, etc.

NLLoc control file statements

NLLoc control file statements calculate earthquake locations in three dimensional space using a nonlinear method.

```
LOCSIG Sissa
```

Identification of individual, institution or other entity. Written in some output files, e.g. in the loc.sum.grid0.loc.hyp file like this: SIGNATURE "Sissa

obs:./obs/Husmuli_2011_2012_w_Polarities.obs

NLLoc:v7.00.00 (27Oct2017) run:31May2020 22h44m12".

```
LOCCOM HUSMULI 2011-2012
```

Comment about location run. Written in some output files, e.g. in the loc.sum.grid0.loc.hyp file like this: COMMENT "HUSMULI 2011-2012".

```
LOCFILES ./obs/Husmuli_2011_2012_w_Polarities.obs NLLoc_OBS  
./time/layer ./loc/LOGGAU2_0.1_0.005_0.5_EDT/loc
```

./obs/Husmuli_2011_2012_w_Polarities.obs = the directory path and filename for the phase or observation files

NLLoc_OBS = the file format of the observation file (all options listed on NLLoc website)

./time/layer = the file root name (no extension) for the input time grids (has to be the same as in commands GTFILES and EQFILES)

./loc/LOGGAU2_0.1_0.005_0.5_EDT/loc = the file root name for the output files. Change this root name in accordance with the settings for the LOGGAU2 command.



```
LOCGRID 201 201 201 -10.0 -10.0 -1.0 0.1 0.1 0.1 PROB_DENSITY  
SAVE
```

This line specifies the size of the 3D search grid. You can have more than one line with the LOCGRID command. The first line is the original grid. Succeeding LOCGRID commands are for nested gridding (which we have not done at ISOR). To get nested gridding you put xOrig, yOrig, zOrig = -1.0e30.

201 = number of grid nodes in the x direction

201 = number of grid nodes in the y direction

201 = number of grid nodes in the z direction

-10.0 = x location of the grid origin in km relative to the geographic origin

-10.0 = y location of the grid origin in km relative to the geographic origin

-1.0 = z location of the grid origin in km relative to the geographic origin

0.1 = grid node spacing in kilometers along the x axes

0.1 = grid node spacing in kilometers along the y axes

0.1 = grid node spacing in kilometers along the z axes

PROB_DENSITY = statistical quantity to calculate on grid (other option is MISFIT)

SAVE = specify that the results of the search over this grid should be saved to disk

The size of our grid is $(201-1) * 0.1 = 20$ km in each direction. Be careful that the grid node spacing doesn't coincide with the spacing in the velocity model.

```
LOCHYPOUT SAVE_NLLOC_ALL SAVE_HYPOINV_SUM
```

Tell the program which filetype to use for the output. You can write as many output types as you want.

All options are listed on the NonLinLoc website.

SAVE_NLLOC_ALL = save summary and event files of type NLLoc Hypocenter-Phase file , Phase Statistics file , Scatter file and Confidence Level file

SAVE_HYPOINV_SUM = save summary file only of type HypoInverse Archive file. The HypoInverse Archive format serves as input to the program FPFIT which is a program for grid-search determination of focal mechanism solutions (Reasenberget al., 1985).

```
LOCSEARCH OCT 40 40 20 0.001 64000 10000 0 1
```

There are three different possible types of searches available in NonLinLoc. We use the Oct-tree method. The oct-tree method is a type of grid search method. Lomax and Curtis call it „oct-tree importance sampling algorithm“ which gives accurate, efficient, and complete mapping of earthquake location PDF in 3D space. It divides the sample space into smaller and smaller cells, always creating 8 cells to sample in the cell which had the highest probability in the previous step. The photo below explains the procedure. It is faster than a full grid-search, more global and complete than a Metropolis-simulated annealing, and is simple. The drawbacks are that the results are weakly dependant on initial grid size and may miss narrow, local maxima in the PDF, and it attempts to read full 3D travel-time grid files into memory which can be slow. Information about oct-tree sampling was found on the nlloc website, <http://alomax.free.fr/nlloc/octtree/OctTree.html>.

Oct-Tree sampling procedure

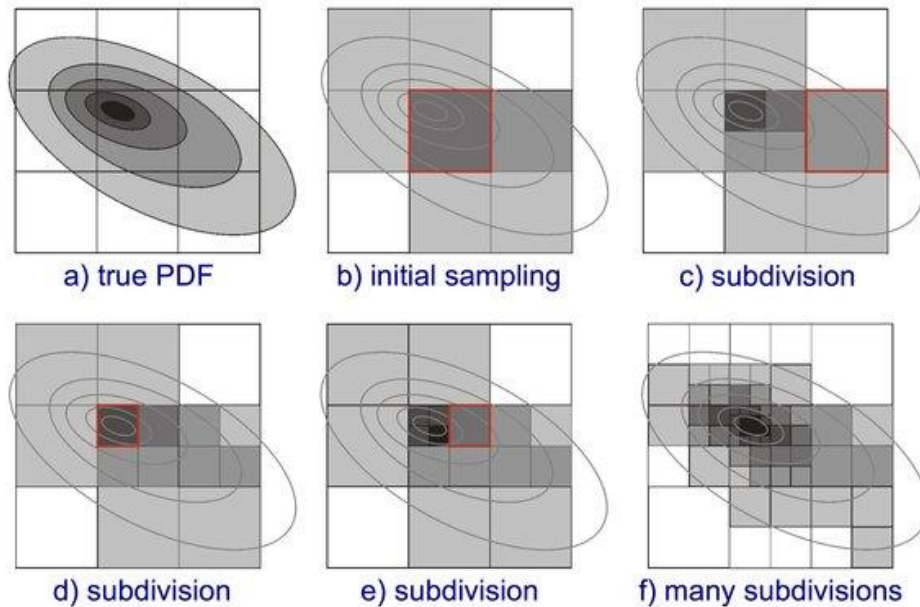


Figure 1 From Lomax and Carter, <http://alomax.free.fr/nlloc/octtree/OctTree.html>

40 = initial number of octtree cells in the x direction

40 = initial number of octtree cells in the y direction

20 = initial number of octtree cells in the z direction

0.001 = smallest octtree node side length to process, the octtree search is terminated after a node with a side smaller than this length is generated

64000 = total number of nodes to process

10000 = the number of scatter samples to draw from the octtree results (scatter samples can be used to plot and represent the PDF of the earthquake location)

0 = (integer, min:0, max:1, default:0) flag, if 1 weights oct-tree cell probability values used for subdivide decision in proportion to number of stations in oct-tree cell; gives higher search priority to cells containing stations, stabilises convergence to local events when global search used with dense cluster of local stations.

1 = (integer, min:0, max:1, default:1) flag, if 1, stop search when first min_node_size reached, if 0 stop subdividing a given cell when min_node_size reached

```
LOCMETH EDT_OT_WT 9999.0 4 -1 -1 -1.68 6 -1.0 1
```

Here we specify which location method (algorithm) to use and define the relevant parameters. In NonLinLoc you can choose from three different types of methods. GAU_ANALYTIC, EDT and EDT_OT_WT. The choice of method can influence the final location. GAU_ANALYTIC uses an L2-RMS misfit function and is sensitive to outlier data (one or a few bad readings can shift the hypocenters significantly). EDT is an equal differential time likelihood function and is not as sensitive to outlier data. EDT_OT_WT weights EDT-sum probabilities by the variance of origin-time estimates over all pairs of readings. This reduces the probability (PDF values) at points with inconsistent OT estimates, and leads to more compact location PDF's.

After recommendation with Anthony Lomax ISOR tried GAU_ANALYTIC instead of EDT_OT_WT because we were trying to compare to locations from VELEST which probably uses an RMS misfit



function. But the difference between locations found with GAU_ANALYTIC and EDT_OT_WT were small.

EDT_OT_WT = RMS misfit function method

9999.0 = maximum distance in km between a station and the center of the initial search grid

4 = minimum number of phases that must be accepted before event will be located

-1 = maximum number of accepted phases that will be used for event location, -1 for no max

-1 = minimum number of S phases that must be accepted before event will be located, -1 for no max

-1.68 = P velocity to S velocity ratio. If VpVsRatio > 0.0 then only P phase travel-times grids are read and VpVsRatio is used to calculate S phase travel-times. If VpVsRatio < 0.0 then S phase travel-times grids are used

6 = maximum number of 3D travel-time grids to attempt to read into memory for Metropolis-Gibbs search. This helps to avoid time-consuming memory swapping that occurs if the total size of grids read exceeds the real memory of the computer. 3D grids not in memory are read directly from disk. If maxNum3DGridMemory < 0 then NLLoc attempts to read all grids into memory.

-1.0 = minimum distance in km between a station and the center of the initial search grid; phases from stations closer than this distance will not be used for event location, -1 for no min.

1 = reject duplicate arrivals (arrivals which have same station label and phase name)

The last parameter was not included when the GAU_ANALYTIC method was tested.

LOCGAU 0.1 0.0

Gaussian model error parameters. They account for errors that pop up because our velocity model is not a perfect description of the real world. Covariance $ij = \text{SigmaTime}^2 \exp(-0.5(\text{Dist}^2 / ij) / \text{CorrLen}^2)$ where Dist is the distance in km between stations i and j

0.1 = typical error in seconds for travel-time to one station due to model errors

0.0 = correlation length that controls covariance between stations (i.e. may be related to a characteristic scale length of the medium if variations on this scale are not included in the velocity model)

LOCGAU2 0.1 0.005 0.5

Specifies parameters for travel-time dependent modelisation-error. Sets the travel-time error in proportion to the travel-time, thus giving effectively a station-distance weighting, which was not included in the standard Tarantola and Valette formulation used by LOCGAU. This is important with velocity model errors, because nearby stations would usually have less absolute error than very far stations, and in general it is probably more correct that travel-time error is a percentage of the travel-time. Preliminary results using LOCGAU2 indicate that this way of setting travel-time errors gives visible improvement in hypocenter clustering. Can currently only be used with the EDT location methods. Different values should be tested for this command. Change the root of the output file in command LOCFILES so that reflects the values chosen for the LOCGAU2 command. Otherwise it would write over the output file making it impossible to compare the output.

0.1 = fraction of of travel-time to use as error

0.005 = minimum travel-time error in seconds

0.5 = maximum travel-time error in seconds

*This seems to have little influence for small networks where the stations are located close (<30-40 km) from the source.

LOCPHASEID P P p G PN PG

LOCPHASEID S S s G SN SG

Specifies the mapping of phase codes in the phase/observation file (i.e. pg or Sn) to standardized phase codes (i.e. P or S).

P/S = standardized phase code (used to generate time-grid file names)

P p G PN PG/ S s G SN SG = one or more phase codes that may be present in a phase/observation file that should be mapped to the standardized phase code



LOCQUAL2ERR 0.1 0.5 1.0 2.0 99999.9

Required for phase/observation file formats that do not include time uncertainties, ignored otherwise. Specifies the mapping of phase pick qualities phase/observation file (i.e. 0,1,2,3 or 4) to time uncertainties in seconds (i.e. 0.01 or 0.5).

0 => 0.1

1 => 0.5

2 => 1.0

3 => 2.0

4 => 99999.9 (large, positive values are used to indicate a phase pick that should have zero weight (infinite uncertain))

LOCPHSTAT 9999.0 -1 9999.0 1.0 1.0 9999.9 -9999.9 9999.9

Specifies selection criteria for phase residuals to be included in calculation of average P and S station residuals. The average residuals are saved to a summary, phase statistics file (see Phase Statistics file formats).

9999.0 = the maximum allowed hypocenter RMS in seconds (default: VERY LARGE DOUBLE)

-1 = the minimum allowed hypocenter number of readings

9999.0 = the maximum allowed hypocenter gap in degrees

1.0 = the maximum allowed residual in seconds for a P or S phase

1.0 = ?

9999.9 = ?

-9999.9 = ?

9999.9 = ?

LOCANGLES ANGLES_YES 5

Specifies whether to determine take-off angles for the maximum likelihood hypocenter and sets minimum quality cutoff for saving angles and corresponding phases to the HypoInverse Archive file.

ANGLES_YES = take-off angles are read from angles grid files and output to locations files

5 = minimum quality for writing take-off angles and corresponding phase to the HypoInverse Archive File (options from 0 to 10, 5 is default)

How to include station delays:

```
LOCDELAY MEI05 P 1 -0.11
LOCDELAY MEI05 S 1 -0.77
LOCDELAY BIT06 P 1 -0.11
...
```

Specifies P and S delays (station corrections) to be subtracted from observed P and S times. We used station corrections from VELEST for locations of earthquakes in Hverahlid. It makes a big difference. The example lines here are from the run in Hverahlid.

Format: LOCDELAY station_name phase number_of_readings delay

MEI05 = station name

P = phase

1 = number of residuals used to calculate mean residual/delay (not used by NLLoc, included for compatibility with the format of a summary, phase statistics file)

-0.11 = delay in seconds, subtracted from observed time



5.0 How to run

To run NonLinLoc you type in these commands in this order into the command line window:

- Vel2Grid7 run/control.in
- comment out command line VGTYPE P and un-comment VGTYPE S
- Vel2Grid7 run/control.in
- Grid2Time7 run/control.in
- comment out line GTFILES ./model/layer.model ./time/layer P and un-comment GTFILES ./model/layer.model ./time/layer S
- Grid2Time7 run/control.in
- NLLoc7
- look at results in file ./loc/LOGGAU2_0.1_0.005_0.5_EDT/loc.sum.grid0.loc.hy

6.0 More information

<http://alomax.free.fr/nlloc/>